Nanoscale

REVIEW

View Article Online
View Journal | View Issue

Cite this: *Nanoscale*, 2023, **15**, 15885

A comprehensive exploration of the latest innovations for advancements in enhancing selectivity of nanozymes for theranostic nanoplatforms

Dan Li, *[a] Tuocen Fan [b] and Xifan Mei*[b]

Nanozymes have captured significant attention as a versatile and promising alternative to natural enzymes in catalytic applications, with wide-ranging implications for both diagnosis and therapy. However, the limited selectivity exhibited by many nanozymes presents challenges to their efficacy in diagnosis and raises concerns regarding their impact on the progression of disease treatments. In this article, we explore the latest innovations aimed at enhancing the selectivity of nanozymes, thereby expanding their applications in theranostic nanoplatforms. We place paramount importance on the critical development of highly selective nanozymes and present innovative strategies that have yielded remarkable outcomes in augmenting selectivities. The strategies encompass enhancements in analyte selectivity by incorporating recognition units, refining activity selectivity through the meticulous control of structural and elemental composition, integrating synergistic materials, fabricating selective nanomaterials, and comprehensively fine-tuning selectivity *via* approaches such as surface modification, cascade nanozyme systems, and manipulation of external stimuli. Additionally, we propose optimized approaches to propel the further advancement of these tailored nanozymes while considering the limitations associated with existing techniques. Our ultimate objective is to present a comprehensive solution that effectively addresses the limitations attributed to non-selective nanozymes, thus unlocking the full potential of these catalytic systems in the realm of theranostics.

Received 10th July 2023,
Accepted 22nd September 2023

DOI: 10.1039/d3nr03327a

rsc.li/nanoscale

1. Introduction

Nanozymes, a captivating class of artificial enzymes, hold tremendous potential across diverse fields, offering significant advantages over natural enzymes, including improved stability, easier synthesis, and customization.[1–3] However, unlike natural enzymes, most nanozymes lack selectivity and can catalyze multiple reactions indiscriminately.[4–7] This characteristic arises from their diverse structures, multiple reactive sites on the surface, abundant redox potential, and non-specific binding to various substrates.[8–23] While their multifunctional enzyme-like properties enable various applications, such as detections, disease therapy, and environmental remediation,[24–37] their non-selective nature poses challenges in certain contexts, particularly for theragnostic nanoplatforms where precise control is crucial. Therefore, the development of more selective nanozymes has become essential to address these limitations and optimize their applications. Various methods have been investigated to boost the activity of nanozymes. For instance, Dong *et al.* demonstrated the development of AFCT (Fe-doped CeO_2 (Fe–CeO_v)) nanozymes modified with (4-carboxybutyl) triphenylphosphonium bromide (TPP) moieties and loading them with 2, 2′-casino-bis(3-ethylbenzothiazoline-6-sulfonic acid (ABTS)) nanozymes, which exhibited superior catalytic activities in multienzyme-mimicking cascade reactions, encompassing superoxide dismutase (SOD), peroxidase (POD), and nicotinamide adenine dinucleotide (NADH) POD-mimics. These enhanced catalytic properties were attributed to the successful integration of critical enzyme-mimicking active sites through defect engineering.[38] Despite these advancements in enhancing enzyme-like activities, the issue of selectivity remains crucial, as non-selective nanozymes may cause interference in analysis, disrupt cellular processes, and lead to potential toxicity.[39–43] To leverage the full potential of nanozymes in theranostics, it is necessary to enhance their selectivity.

Previous reviews have shed light on enhancing the catalytic activities, discussing mechanisms, synthesis methods, and applications of nanozymes.[44–56] However, some of these

[a]*College of Pharmacy, Jinzhou Medical University, 40 Songpo Rd, Jinzhou 121000, China. E-mail: danli@jzmu.edu.cn*
[b]*Jinzhou Medical University, 40 Songpo Rd, Jinzhou 121000, China. E-mail: meixifan@jzmu.edu.cn*

reviews have only offered partial insights into selectivity enhancement, while others have not sufficiently underscored the significance of reaction selectivity within the broader context of the subject matter. A few reviews have indeed delved into summarizing selectivity enhancement. For instance, Somerville *et al.* explored methods such as active site regulation and the creation of nanoconfined substrate channels around these meticulously controlled active sites to heighten selectivity.[56] Li *et al.* addressed advancements in catalytic selectivity through techniques like molecular imprinting, nanoenzyme cascade reactions, and the integration of nanozymes with additional recognition elements for analytical purposes.[55] Nonetheless, it is worth noting that these works in the field still fall short of providing a comprehensive treatment of selectivity modification strategies, which is crucial for their effective utilization in theranostics.

Not only can analyte selectivity be improved by incorporating recognition elements, but activity selectivity can also benefit from the introduction of specific sites through distinct structural and compositional features. To further elevate both the activity and selectivity of nanozymes, synergistically integrating various materials has proven to be a viable approach. Moreover, tailoring the physicochemical properties of nanomaterials provides an effective means to engineer selective nanozymes. A multitude of strategies is available to enhance various selectivities, encompassing analyte, activity, and substrate selectivities. Surface modification emerges as a pivotal strategy for achieving selective nanozymes, as it can influence both the active site and recognition ability. Furthermore, the strategic utilization of external stimuli, such as light, pH, and temperature, offers an effective means to fine-tune activity selectivity, thereby enhancing substrate or analyte selectivity. Another promising approach involves the use of cascade nanozyme systems, designed to mimic natural enzymatic cascade reactions. This approach allows for precise control over reaction pathways while minimizing the generation of undesired byproducts. These diverse strategies can be applied individually or in synergy, and their exploration is of paramount importance for advancing the development of tailor-made selective nanozymes for theranostic applications. Our exploration extends to novel strategies highlighted in recent publications, where we delve deeper into the discourse surrounding nanozyme selectivity modification. Moreover, we broaden our perspective to explore the potential applications of these strategies in theragnostics, accompanied by a comprehensive examination of their broader implications. In summary, we emphasize the latest strategies (as depicted in Fig. 1) designed to improve selectivity, encompassing activity, substrate, and analyte selectivity, while also considering additional factors that can comprehensively enhance their performance. By underlining the significance of selectivity improvement in nanozymes, our objective is to inspire new research directions and promote the efficient, safe, and selective catalysis of diverse chemical reactions for the simultaneous diagnosis and treatment of various diseases.

2. Nanozymes for theranostic nanoplatforms

Theranostic platforms represent a groundbreaking paradigm in healthcare, merging diagnostic and therapeutic capabilities

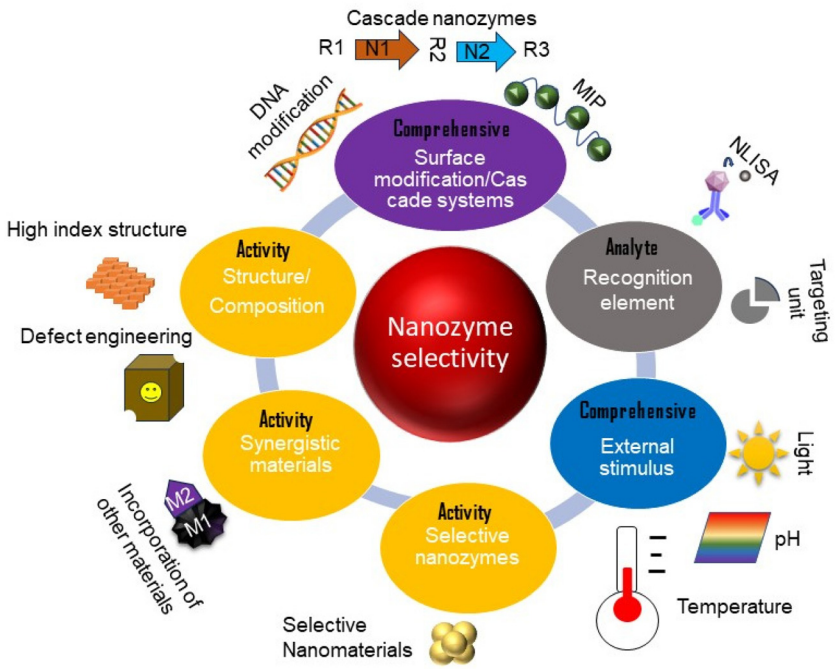

Fig. 1 Schematic representation of recent endeavors aimed at enhancing the selectivity of nanozymes.

to provide tailored, effective, and minimally invasive treatments. The integration of nanozymes into theranostic nanoplatforms holds the potential for a profound transformation in healthcare. Nanozymes harness their unique optical properties to facilitate precise imaging and a diverse array of optical assays for detecting biomarkers, cells, or lesions associated with a broad spectrum of diseases.[57] In addition to their catalytic capabilities, they may activate prodrugs to generate therapeutic substances for disease treatment.[58] Nanozymes can also serve as effective drug carriers.[59–61] This versatility expands their applications in medical interventions.

To further highlight the remarkable potential of nanozyme-based theranostic platforms, Table 1 is referenced below, providing compelling examples of their capabilities in treating animal models. For example, a responsive bismuth-manganese-based nanozyme (BDS-GO_x@MnO_x) was created using the dopamine hydrochloride (DOPA)/bovine serum albumin (BSA) oil–water method.[62] This nanozyme effectively treats tumors and enhances imaging through computed tomography (CT) and magnetic resonance imaging (MRI) of mice. Additionally, a 2D vanadium carbide (V_2C) MXene nanozyme, designed to mimic natural enzymes such as SOD, POD, catalase (CAT), and glutathione POD (GPx),[63] effectively reducing oxidative stress while diminishing cerebral infarct volumes and protecting neurons in mice. Furthermore, it serves as a *T*1-weighted MRI contrast agent, enhancing its utility. A one-step microwave-assisted method yields carbon dots (C-dots) nanozymes that exhibit mitochondrion-specific properties that enhance therapy and facilitate real-time monitoring as they move from the mitochondrion to the nucleolus. Similarly, some other C-dots nanozyme, with SOD-like activity, not only participate in bioimaging but also venture into therapeutic intervention, offering relief for conditions like Acute Lung Injury (ALI) in mice through ROS scavenging.[18,64]

Table 1 Typical examples of nanozyme-based theranostic platform

System	Nanozyme	Activity	Diagnosis	Therapy	Ref.
BDS–GO_x@MnO_x	MnO_x	Multi-oxidoreductase	Tumor-enhanced CT and MR imaging	Ablation of malignant tumors	62
FeCu–GO_x PNzyme-MTO	FeCu PNzyme	POD	Enhanced IR/MR/FL imaging of tumor ablation	Multimodal tumor therapy	69
FTRNPs	Fe_3O_4 nanoparticles	POD	PAI of tumor	Tumor-specific photo-CD	70
V_2C MXene	V_2C MXene	CAT, SOD, GPx	*T*1-Weighted MRI of ischemia stroke	Ischemic stroke treatment	63
Fe(II)Pc-A	Fe(II)Pc	POD, OXD, CAT	PAI of tumor	PTT for tumor therapy	71
CDs	CDs	OXD, POD	*In situ* visualization of the apoptosis process	Modulation of cancer cell ablation	64
AgPd PB	AgPd PB	CAT, POD	FL imaging, CD, PAI of tumor	PTT for TME	72
MFC-Gem	MFC	POD, GPx	MRI of the PDAC treatment	CD for anti-PDAC therapy	73
AMP NRs	MIL-100	POD	PAI of tumor	PTT-assisted tumor therapy	65
Pt NPs–PVP	Pt NPs–PVP	CAT, POD, SOD	PAI of the kidneys	Treatment of AKI	66
Lipo-OGzyme-AIE	OGzymes	CAT	IVIS imaging of tumor	PDT-assisted tumor therapy	74
Rh-PEG NDs	Rh-PEG NDs	CAT, SOD	PAI	PTT-assisted tumor therapy	67
ACD	Gold nanoclusters	OXD, POD	TME-activated fluorescence imaging	Tumor-specific CDT therapy	75
Janus-CPS	CeO_2–Pt	ROS scavenging enzyme-like activities	NIR-II fluorescent imaging of RA	RA therapy	76
ACP–Fe@D NCs	Fe_3O_4	POD	*In vitro* and *in vivo* magnetic resonance imaging	Enhanced PTT and CDT for tumors	77
C-dots	C-dots	SOD	Bioimaging and ALI treatment	Ameliorating ALI	18
RSPN	CeNZ	CAT, SOD	Photoacoustic ROS imaging	Therapy of acute liver failure	68

AMP NRs, activatable nanozyme-mediated ABTS loaded ABTS@MIL-100/poly(vinylpyrrolidine) (AMP) nanoreactors (NRs); ABTS, 2,2′-azino-bis(3-ethylbenzothiazoline-6-sulfonic acid); PTT, photothermal therapy; MIL-100, MIL-100 belongs to metal–organic frameworks (MOFs), which encompass a group of crystalline materials formed by the coordination of metal ions or clusters with organic ligands; Pt NPs–PVP, polyvinylpyrrolidone-coated platinum nanoparticles; OGzyme, MnO_2 nanoparticles inside the hollow cavity of ferritin nanocages (FTn); Lipo-OGzyme-AIE, OGzymes were encapsulated into phospholipid bilayers and the inner cavity of liposome nanocarriers, respectively; Rh-PEG NDs, polyethylene glycol (PEG)-coated (PEGylated) ultrasmall rhodium nanodots; CDT, chemodynamic therapy; ACD, Cu^{2+}-doped ZIF-8 loaded with gold nanoclusters and doxorubicin hydrochloride (DOX); Janus-CPS, a Janus platform composed of CeO_2–Pt nanozyme and periodic mesoporous organosilica (PMO) subunit on different sides; ACP–Fe@D NCs, ABTS and camptothecin (CPT) are encapsulated into pore-sized dendritic macroporous silica coated Fe_3O_4 nanocapsules, further modified with PVP; NIR-II, second near-infrared window; TME, tumor microenvironment; RA, rheumatoid arthritis; AKI, acute kidney injury; ALI, acute lung injury; PAI, photoacoustic imaging; RSPN, ROS-sensitive nanozyme-augmented PA nanoprobe, which was fabricated by integrating zinc phthalocyanine (ZnPc) and ceria nanozyme (CeNZ). FTRNPs, assembling of Fe_3O_4 nanoparticles, TMB and the RGD peptide; 2D, two-dimensional; V_2C, vanadium carbide; Fe(II)Pc-A, iron phthalocyanine (Fe(II)Pc) was assembled with poly(L-lactide-*co*-glycolide)-*block*-poly(ethylene glycol) to prepare a Fe(II)Pc assembly; AgPd PB, AgPd plasmonic blackbody nanozyme; MFC, $MnFe_2O_4$-loaded carbonaceous nanoparticles loaded with gemcitabine (Gem) (MFC-Gem); PDAC, pancreatic adenocarcinoma.

Beyond these examples, various other animal experiments have demonstrated the potential of nanozymes in theranostics. The intricate interplay within activatable nanozyme-mediated ABTS-loaded ABTS@MIL-100/poly(vinylpyrrolidine) (AMP) nanoreactors (NRs) enhances the precision of photoacoustic imaging (PAI) and drives the effectiveness of photothermal therapy (PTT) by skillfully regulating H_2O_2.[65] Similarly, the Pt NPs-PVP nanozyme exhibits CAT, POD, and SOD functions, making it suitable for PAI for renal assessment while addressing acute kidney injury (AKI) by modulating ROS.[66] Equally significant is the combination of CAT and SOD in polyethylene glycol (PEG)-coated (PEGylated) ultrasmall rhodium nanodots (Rh-PEG NDs), enabling their dual capabilities in PAI and PTT.[67] As well as this, the symphony of the RSPN nanozyme, fabricated by integrating zinc phthalocyanine (ZnPc) and ceria nanozyme (CeNZ) through the amphiphilic ROS-sensitive diselenide (–Se–Se–)-containing polymer (DSeP), heralding the era of Photoacoustic ROS imaging and delivering hope in the nuanced realm of acute liver failure therapy.[68]

These breakthroughs underscore the immense potential of nanozymes in the realm of theranostics, spanning their utility from diagnostics to therapeutic applications.[62] They offer the prospect of propelling precision medicine forward by leveraging multifunctional nanozymes. However, despite encouraging outcomes in preclinical studies, the process of translating these findings into approved clinical treatments is an ongoing endeavor. A significant concern lies in the possibility of side effects resulting from non-selective treatments, which underscores the need for further research and development to fully harness their selective mechanisms.

3. Analyte/target selectivity

To achieve precise targeting of a specific analyte, effective methods involve recognition elements, such as antibodies, aptamers, DNA strands, peptides, or some small ligands, securely affixed with the nanozyme are effective.[78] The nanozymes can be combined with the recognition unit through both covalent binding and non-covalent binding, depending on the specific method and recognition elements used.[79] Covalent conjugation is typically chosen for applications where stability and durability are essential, while non-covalent methods are preferred when preserving functionality and minimizing structural perturbation are priorities. For instance, some antibodies can be conjugated to the nanozyme surface, employing cross-linking agents to realize covalent binding.[80] Non-covalent binding for the conjugation of antibodies to nanozymes can be achieved through several methods, often relying on electrostatic interactions, hydrophobic interactions, or antibody adsorption onto the nanozyme surface.[81] To prevent nonspecific binding events, any remaining unreacted sites on the nanozyme surface are blocked, and binding conditions, including parameters such as pH and temperature, are refined to optimize selectivity.

It's worth noting that nanozyme-linked immunosorbent assay (NLISA) represents a notable application where nanozymes serve as catalytic labels, replacing conventional enzyme labels.[82] In NLISA, nanozymes show analyte selectivity that generates detectable signals, enabling the precise identification of targets. The process may involve immobilizing capture antibodies onto a solid surface, such as a microplate, to capture the targets (Fig. 2). Then, detection antibodies conjugated to nanozymes can also be introduced, leading to the formation of a complex where the target is captured.

NLISA offers several advantages over traditional enzyme-linked immunosorbent assay (ELISA). The catalytic amplification provided by nanozymes enhances the sensitivity of the assay, allowing for the detection of even low concentrations of targets. Additionally, the unique catalytic properties of nanozymes can result in reduced background noise and improved signal-to-noise ratios, enhancing the assay's specificity.[83] The flexibility to choose from various detection methods adds versatility to NLISA, making it adaptable to different experimental setups and sample types.[84,85] For instance, Li *et al.* devised an innovative method named the nanozyme-linked immunosorbent surface plasmon resonance (nano-ELISPR) biosensor, designed for highly sensitive cancer biomarker detection.[86] They integrated a cost-effective nano cup sensor with gold platinum nanoflowers (Au@Pt NFs), known for their POD-like activity. Within this system, the metal substrate effectively triggers MetaSPR signals, while the nanozyme plays a crucial role in catalyzing the formation of oxTMB. A strategically designed chip features surface functionalization with a polydopamine (PDA) film to immobilize alpha-fetoprotein antibody (AFP C-Ab), harnessing PDA's mussel-inspired adhesive properties to initiate a Schiff base reaction with antibody amino residues. Additionally, the incorporation of nanozyme-labeled antibodies accelerates reaction kinetics, thereby boosting the biosensor system's overall performance. Wei *et al.* introduced FeNC–PdNC, an innovative type of Fe single-atom nanozymes (SANs), employing Pd nanoclusters (PdNC) as "modulators" to amplify POD-like activity.[87] FeNC–PdNC acted as a positively

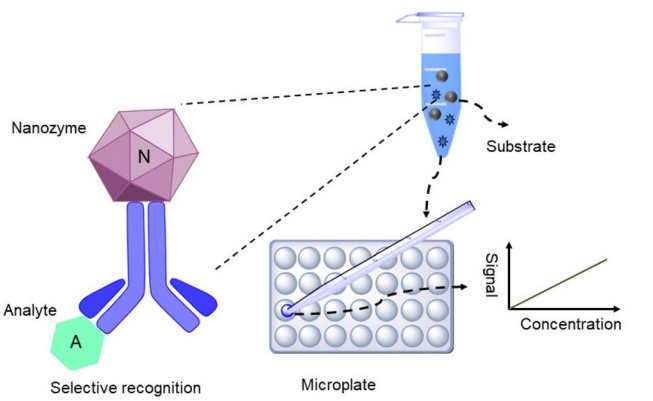

Fig. 2 Graphical representation of direct NLISA for selective recognition of analytes.

charged label conjugated with the PSA antibody (Ab_2) *via* electrostatic interaction. FeNC–PdNC NLISA demonstrated an impressive 0.38 pg mL^{-1} limit of detection (LOD), surpassing HRP-based ELISA. Polina Ivanova *et al.* synthesized noble metal-decorated magnetic nanocubes (MDMCs) for C-reactive protein (CRP) detection through a one-step sandwich NLISA.[88] This NLISA outperformed classical ELISA in sensitivity (LOD = 0.336 ng mL^{-1}), recovery (98.0%), and interference resistance.

While NLISA does offer valuable capabilities, it is important to acknowledge its limitations, including sensitivity challenges, specificity concerns tied to antibody selection, complexities in dealing with intricate sample matrices, and cost considerations. To enhance selectivity in NLISA, one can employ the integration of multimodal detection approaches, signal amplification techniques, refined sample preparation protocols, utilization of advanced nanozyme designs, and the implementation of rigorous quality control measures. These strategies may collectively contribute to heightened specificity and a reduced risk of false outcomes, fortifying NLISA as a robust and dependable method, particularly in the field of theranostics.

Much like NLISA, numerous other recognition units have been incorporated in assay development, utilizing similar covalent or noncovalent approaches. Wang *et al.* embarked on a study to harness the potential synergies between nanobodies and nanozymes, with the overarching aim of enhancing the specificity and sensitivity of immunoassays.[89] The distinctive configuration and diminutive dimensions of nanobodies endow them with the ability to discern epitopes that pose challenges for full-length antibodies to recognize. These nanobodies hold the potential to expedite the creation of exceptionally discerning nanozymes tailored for specific analytes. Zhang *et al.* developed an Au@Pt nanozyme mimicking POD for the analysis of 3-phenoxybenzoic acid (3-PBA).[90] They attached anti-3-PBA nanobodies to Au@Pt-Nbs *via* electrostatic adsorption, enabling selective detection in a lateral-flow nanozyme immunoassay with a cutoff value of 0.005 ng mL^{-1} determined using Adobe Photoshop CC. Nanobodies, characterized by their compact size and remarkable stability, offer valuable support to nanozymes in recognizing challenging epitopes. However, a notable challenge lies in their current limitations in detecting small molecules within complex matrices such as food and biological samples, primarily due to interference issues. Addressing this limitation requires substantial improvements, particularly in the context of analyzing low-concentration contaminants. The inherent solvent may facilitate the selective detection of small molecules following pre-concentration steps.

Incorporating recognition units during the synthesis of nanozymes is another versatile strategy that enables precise control over target selectivity and catalytic activity. For instance, the incorporation of chiral units into covalent organic frameworks (COFs) enables the realization of stereocontrol in enantioselective applications. Zhou *et al.* designed a chiral COF nanozyme with highly ordered active centers.[91] The incorporation of an iron 5,10,15,20-tetrakis(4′-tetraphenylamino)porphyrin unit (Fe-ATPP) and L-Histidine (L-His) modification allows for POD-like activity and enantioselectivity in the oxidation of dopa enantiomers. These chiral modifications expand the applications of nanozymes in theranostics involving chiral molecules or pathways.

4. Activity selectivity improvement

4.1 Synergistic materials

The selectivity of a system is greatly impacted by the synergistic materials it incorporates. While they ensure stability and operational efficiency, they also play a vital role in upholding the overall structural integrity and coherence of the system. For instance, by combining Co_3O_4 and Fe_3O_4 NPs, the resulting shell structure can lead to enhanced activity selectivity due to improved electron transfer and increased surface area. The shell structure can also provide a protective environment for the active sites, resulting in improved stability and longevity of the nanozyme catalyst. The inner Co_3O_4 shells and outer Co–Fe oxide shells served as active sites, while the confined nanoreactor created a locally high content of intermediate products. The integrating Co_3O_4@Co–Fe oxide double-shelled nanostructures (DSNCs) resulted in specific POD-like and faint oxidase (OXD)-like activities (Fig. 3a).[92] Additionally, Co_3O_4@Co–Fe oxide DSNCs showed higher reaction rates for TMB oxidation than single-shelled counterparts due to their peculiar structure and synergistic effect, which can be used to sensitively and selectively detect H_2O_2. Chen *et al.* developed Fe_{SA}–Pt_C by incorporating Pt clusters onto the atomically dispersed Fe–N–C support with hierarchically porous structures (Fig. 3b).[93] The integrating Fe_{SA}–Pt_C exhibits more excellent POD-like selectivity than Fe single atoms (Fe_{SA}) and Pt clusters (Pt_C) nanozymes, which is attributed to the synergy effect as well as the hierarchically porous structure. Liang *et al.* show that integrating substrate-recognition nanomaterials such as C-dots (CDs) with PtNPs can create highly specific POD-like nanozymes (CDs@PtNPs).[94] The enhanced POD-like selectivity facilitated specific bacterial inactivation and biofilm eradication.

Synergistic materials have the potential to enhance the activity selectivity. However, this approach may also pose a risk of reducing their catalytic activity due to the introduction of additional materials, or other agents. Factors such as the choice of materials, as well as the integrating structure and synthesis methods, all influence the selectivity and performance of the integrating nanozymes. Thus, further research and development is necessary to optimize these strategies.

4.2 Structure/composition modification

Through alterations in the physical attributes, structures, and chemical composition of nanozymes, researchers can effectively augment their activity selectivity. For example, Lian *et al.* utilized various agents to finely adjust the Ni/Co ratio of $NiCo_2S_4$ nanoparticles, thereby achieving distinct POD-like activities and selectivities.[95] They observed that the presence of PVP facilitated $NiCo_2S_4$ nanoparticles with a higher Ni/Co ratio compared to $NiCo_2S_4$ (CTAB) nanoparticles, ultimately

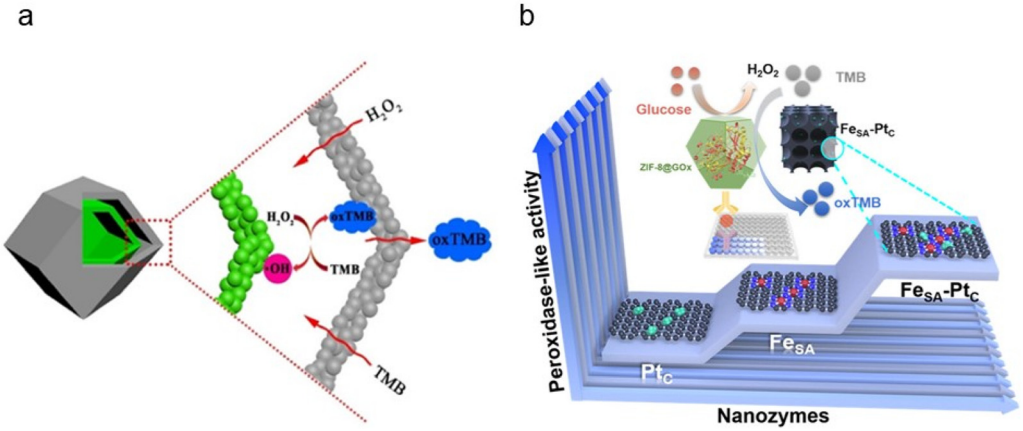

Fig. 3 (a) Schematic representation of Co_3O_4@Co–Fe oxide DSNCs' POD-like activity. Adapted with permission from ref. 92. Copyrights 2023, Elsevier. (b) Enhanced POD-like activity colorimetric immunoassay *via* Fe_{SA} coupled with Pt_C.[93] Copyrights 2021, ACS.

resulting in the nanozymes exhibiting enhanced POD-like selectivities. Furthermore, numerous other strategies have been employed to influence the structure and composition of nanozymes, to modify their selectivities.

4.2.1 High-index nanozymes. The activity selectivity of high-index nanozymes can be significantly different from that of their low-index counterparts due to the unique atomic arrangements on their surfaces and some molecules can selectively adsorb onto the high-index plane of the metal surface.[96] Tang *et al.* discovered a highly efficient intermetallic compound, known as H-Pt_3Sn, which exhibited excellent POD-like activity and specificity.[97] H-Pt_3Sn has a unique structure with evenly distributed Pt and Sn and a (540) terrace step indicated by TMB assay (Fig. 4a and b). It demonstrates excellent catalytic specificity towards H_2O_2 activation and very low OXD-like and CAT-like activities. Xu *et al.* also enhanced activity selectivity using high-index nanozymes.[98] They engineered gold nanorods (Au NRs) induced by Cu^{2+} to form high-index {200} facets (Fig. 4c). These specially designed Au/Cu NRs exhibited increased charge density at specific locations owing to their high-index facets, which facilitated efficient electron transfer to H_2O_2 and resulted in enhanced POD-like properties. The catalytic efficacy of these Au/Cu NRs demonstrated a remarkable 4.5-fold increase in catalytic activity compared to low-index Au NRs. High-index nanozymes enhance the selectivity of nanozymes by offering new functionalities due to their distinct physical and chemical properties. However, as the number of facets increases, the surface area also increases, which can lead to instability and degradation. Controlling the morphology and size of high-index nanozymes can be difficult, leading to variations in their properties and performance. Thus, further research may be required to control the selectivity of high-index nanozymes.

4.2.2 Defect engineering. The introduction of defects through various methods, such as creating vacancies, incorporating binding sites, or designing SANs with vacancies (Fig. 5), can lead to several advantageous effects. These effects may include the creation of new active sites, an increase in surface area, and the introduction of new functionalities, all of which collectively contribute to enhancing catalytic selectivity.

4.2.2.1 Vacancy introduction. Vacancies can be created by intentionally removing or adding atoms or by altering the crystal structure of the nanozymes. Amorphous materials have disordered features that can provide catalytically active defects and unsaturated atoms on their surfaces. For instance, Zhang *et al.* created a vacancy-rich monolayer nanosheet (m-CoAl-LDH) with higher SOD-like activity for mitigating mitochondrial oxidative damage.[99] The m-CoAl-LDH's monolayer structure and numerous vacancies resulted in high activity in specifically decomposing $O_2^{\bullet-}$ into H_2O_2 and O_2. Shang *et al.* synthesized amorphous/crystalline PtRuTe nanozymes with abundant amorphous domains, resulting in highly efficient POD-like selectivity.[100] The highly amorphous PtRuTe nanozymes show much higher POD-like activities than their crystalline counterparts, with remarkable enzymatic specificity and suppressed OXD-like activities. Lu *et al.* enhanced oxygen vacancies (OVs), which resulted in increased oxygen storage capacity and OXD-like activity, promoted the presence of lower-valence Mn species (as illustrated in Fig. 6a).[101] In particular, OV-Mn_3O_4 outperforms Mn_3O_4 Nanoflowers (NFs) in the detection of L-cysteine, offering a significantly lower detection limit (1.31 μM *vs.* 5.69 μM).[102] Additionally, Song *et al.* synthesized OVs-rich manganese oxide (OVs-Mn_2O_3-400) by pyrolyzing an Mn(II)-based metal–organic gel precursor. OVs-Mn_2O_3-400 exhibited robust OXD-like activity, leveraging oxygen vacancies to produce $O_2^{\bullet-}$ (Fig. 6b). These vacancies may influence reaction pathways, kinetics, and the stabilization of intermediates, allowing for the selective enhancement of catalytic activity towards specific reactions or substrates. Additionally, synergistic effects may arise when vacancies are combined with other catalytic materials, further optimizing both activity and selectivity. In essence, vacancies offer a versatile means to fine-tune nanozyme properties, making them more efficient and selective for applications.

4.2.2.2 Incorporation of active sites. By introducing active sites, such as transition metals, nonmetals, certain center structures, or ligands into nanozymes, it is possible to modify

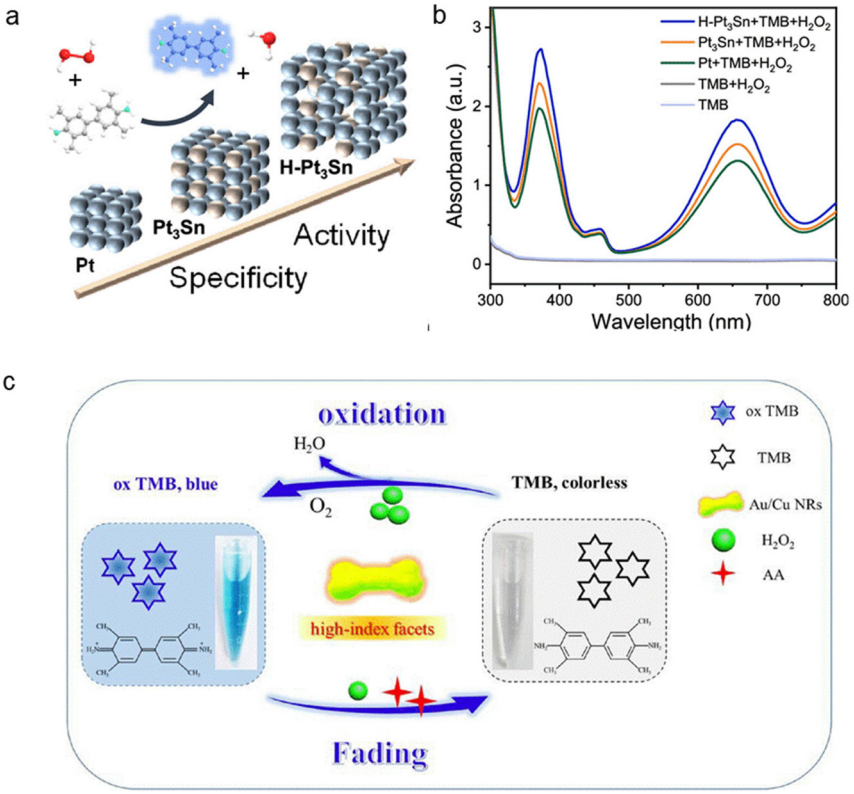

Fig. 4 (a) POD-like activity of nanozymes with different structures. (b) Different levels of absorbance were observed for the H_2O_2-TMB system in the presence of different nanozymes, with the order being H-Pt_3Sn > Pt_3Sn > Pt. Adapted with permission from ref. 97. Copyrights 2023, ACS. (c) Preparation and application of high-index Au/Cu NR for colorimetric assay using TMB-oxTMB system for detection of ascorbic acid (AA). Adapted with permission from ref. 98. Copyrights 2019, Elsevier.

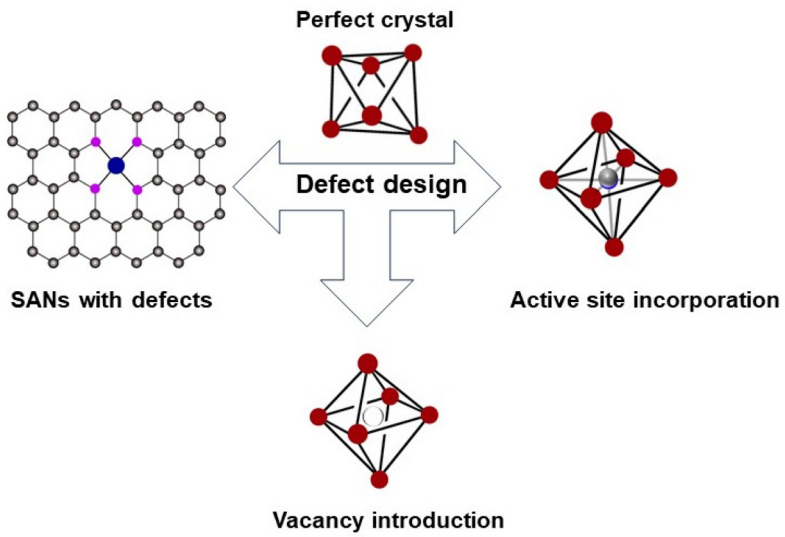

Fig. 5 Defect engineering by introducing vacancies, active sites, and the design of SANs with defects.

their electronic and structural properties and create new active sites for catalysis. These sites can improve the activity selectivity of the catalytic reaction by bringing the substrate molecules close to the active site of the nanozymes.

Nitrogen (N) doping can be a general strategy to enhance the POD-mimicking activities of carbon-based materials such as carbon nanotubes and graphene by modifying their electronic properties and surface chemistry.[103] Ye *et al.* introduced

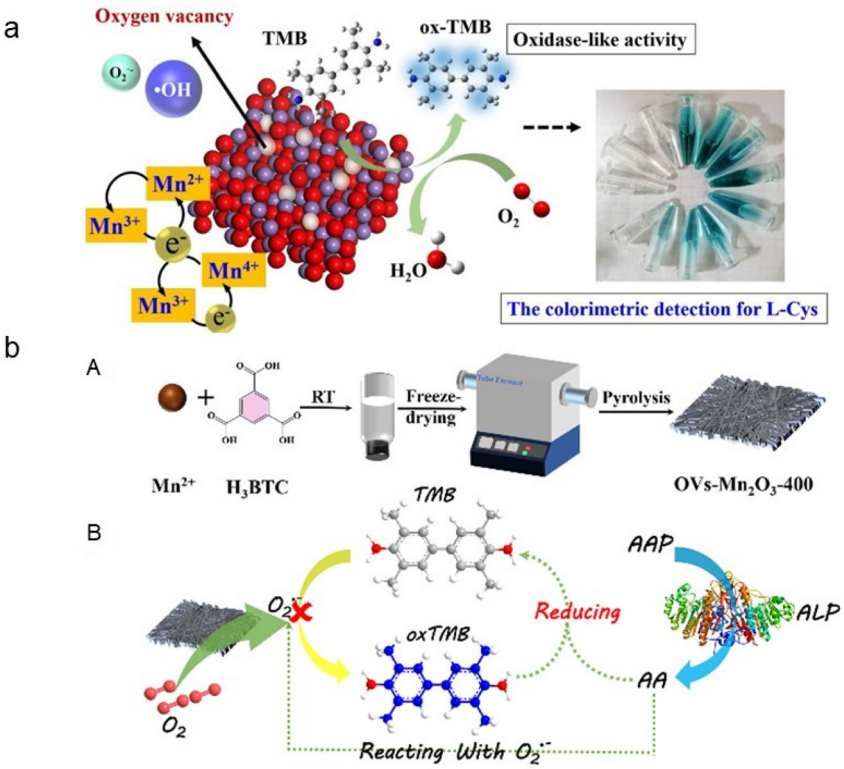

Fig. 6 (a) OVs modulation Mn_3O_4 nanozyme with enhanced OXD-mimicking performance for L-cysteine detection. Adapted with permission from ref. 101. Copyrights 2021, Elesver. (b) Preparation of OVs-Mn_2O_3-400 (A) and the colorimetric sensor for ALP detection (B). Adapted with permission from ref. 102 Copyrights 2023, ACS.

a method for preparing a nanozyme named HBF-1-C800, which was an N-doped carbon material with a porous structure.[104] The authors used a high-temperature pyrolysis process to prepare this material, resulting in a high N-doping efficiency of 5.48%. HBF-1-C800 nanozyme is highly stable and displays a 3- to 7-fold improvement in POD-like activity compared to conventional carbon nanozymes and a 5-fold improvement compared to the reported N-doping graphene. Moreover, the HBF-1-C800 nanozyme showed negligible activities for OXD, CAT, and SOD, indicating a highly specific property. This specific activity is essential for designing accurate biosensors and was further utilized for sensing biomarkers such as hydrogen peroxide, glutathione, and glucose. Hu *et al.* found that N-doping in reduced graphene oxide (rGO) significantly boosted its POD-mimicking activities while also achieving exceptional specificity.[105] N-rGO selectively activates H_2O_2 rather than O_2 and $O_2^{\bullet-}$ by forming and stabilizing radical oxygen species near the N sites of N-rGO. These radical oxygen species then oxidize POD substrates, leading to the specific POD-mimicking activity of N-rGO.

The addition of other elements such as phosphorus (P) heteroatom to Fe–N–C SANs improves their POD-like activity.[106] Boruah *et al.* synthesized a 1D carbon nanowire catalyst (FeNCP/NW), with enriched Fe–N_4 active sites, and P atoms are doped into the carbon matrix to affect the Fe center through long-range interaction. P-doping significantly enhances the POD-like activity, with excellent selectivity and stability. Furthermore, FeNCP/NW is used for highly sensitive colorimetric detection of acetylcholine in an enzyme cascade platform.

Metal doping can also improve the selectivity of nanozymes by introducing new active sites and altering their electronic properties. For example, metal elements such as Fe, Ni, Bi, and Cu are known to be useful in enhancing POD-like selectivity.[107] Au, Co, Ce, Cd, and Pt may enhance the CAT-like activity,[108] which may be useful in the removal of H_2O_2 and other oxidants. Wang *et al.* found doping Cu aerogel with bismuth (Bi) at a 9 : 1 CuBi ratio improved its POD-like activity compared to the undoped aerogel.[109] Compared to CeO_2, M/CeO_2 showed significantly improved POD-like activity (8–10 fold), with Mn/CeO_2 showing superior SOD-like activity and Co/CeO_2 exhibiting high selectivity towards CAT-like activity.[110] Cheng *et al.* developed a strategy to directly construct highly efficient 1D sub-nanochannels within Fe-based (MIL-53(Fe)) nanozymes.[111] Ni-doping and H_2-treatment generated Ni^{II} and mixed-valence Fe^{II}/Fe^{III} nodes in the 1D iron oxide octahedral chains to act as adsorption and reversible catalytic sites of H_2O_2, respectively. Ni_xFe-MOF-based nanozymes exhibited high activity, sensitivity, and selectivity toward H_2O_2 (Fig. 7a and b) and glutathione (GSH) detection. The Fe^{II}/Fe^{III} reversible catalytic and Ni^{II} adsorption sites worked synergistically, leading to the formation of more coordinated unsaturated

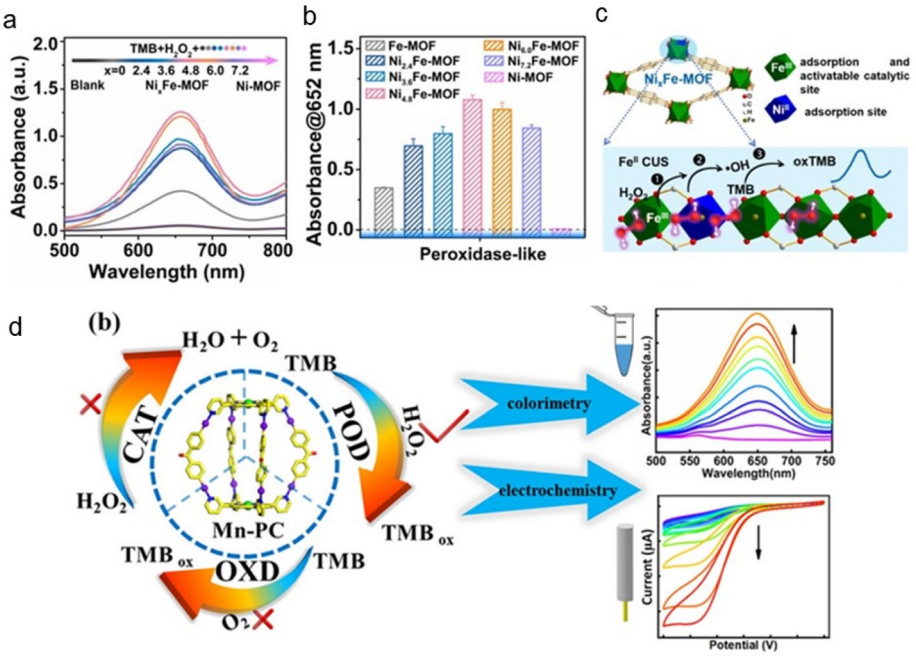

Fig. 7 (a) The POD-like activities of Ni_xFe-MOFs (x = 0, 2.4, 3.6, 4.8, 6.0, and 7.2) were evaluated by the TMB + H_2O_2 assay. (b) Comparison of POD-like activities of Ni_xFe-MOF nanozymes. (c) A proposed mechanism of how bimetallic Ni_xFe-MOF nanozymes activate both catalytic and adsorption sites. Adapted with permission from ref. 111. Copyrights 2022, Elsevier. (d) Metallacages incorporating precise porphyrin-based active sites through the self-assembly of PC, Zn-PC, and Mn-PC complexes, with subsequent applications in colorimetric and electrochemical biosensing utilizing Mn-PC. Adapted with permission from ref. 112. Copyrights 2022, ACS.

sites (CUSs) and accelerating substrate transport (Fig. 7c). However, excess Ni^{II} adsorption sites reduced Fe activatable catalytic sites, thereby reducing catalytic activities. This strategy could potentially be used for designing highly selective MOF-based nanozymes. Zhou *et al.* employed the coordination-driven self-assembly methodology to fabricate an Mn (III)-containing supramolecular nanocage named Mn-PC (Fig. 7d), given the role of coordinated metal ions with variable valence states as the active center of enzymes.[112]

Mn-PC manifested enhanced POD-like activity selectivity compared to the previously reported porphyrin cage (PC) and zinc porphyrin cage (Zn-PC). Mn-PC solely demonstrated POD-mimicking activity, and its cage-like configuration facilitated a uniform microenvironment for the active sites, analogous to the intricate scaffolding of natural enzymes. Thus, Mn-PC exhibited selective POD-like activity, precluding any OXD-like or CAT-like characteristics. A MOF-818 nanozyme was modified to include trinuclear Cu centers that exhibit exceptional selectivity, much like the natural catechol OXD activity.[113] During the catalytic cycle, O_2 was required to reoxidize copper (I), while H_2O_2 was produced gradually in a rate-determining step. Compared to previously reported catechol nanozymes, it outperforms their catechol OXD selectivity.

Overall, introducing active sites can improve the selectivity of nanozymes and enhance their potential for specific applications. However, incorporating foreign sites into the lattice or surface of nanozymes may alter their morphology, size, and crystallinity, leading to variations in their properties and performance. The distribution of active sites can also be uneven, creating regions with different catalytic activity. The effectiveness in improving selectivity depends on the intrinsic properties of the nanozymes, the dopant selection, and the catalytic mechanism involved. Therefore, it is essential to carefully optimize the synthesis and functionalization of the material to achieve the desired selectivity.

4.2.2.3 Construction selective SANs with vacancies. SANs can potentially have defects, which are irregularities or imperfections in their atomic or molecular structure arising from factors such as the synthesis process, environmental conditions, or inherent material properties. These defects in SANs, including missing atoms, surface imperfections, and coordination irregularities, can influence their catalytic activity. The missing atoms within their atomic structure can impact their catalytic efficiency, while surface defects may alter their surface reactivity and catalytic properties. The coordination of the single atom with the support material can also affect activity selectivity, and suboptimal coordination can be considered a defect. For instance, Chen *et al.* developed a flower-like single copper site (CuN_3) nanozyme (Cu SSN) with exceptional activity and specificity to oxidize phenols using solid migration.[114] When abundant CuN_3 was engaged, the specific activity of Cu SSN was found to be nine times greater than that of laccase, and it demonstrated remarkable stability even in challenging environmental conditions. Yang's group developed Cu SAs/CN nanozyme with active $Cu–N_4$ moieties, which exhibited comparable ascorbate POD (APX) mimetic

activity and fast kinetic to natural APXs.[115] Cu SAs/CN's superior APX-like activity comes from the electron transfer process between single Cu atoms and coordinated N atoms, which activates absorbed H_2O_2 and leads to facile cleavage. Additionally, Cu SAs/CN outperforms natural APXs in terms of robustness and selectivity. The results provide insight into the APX-like reaction process for nanozymes and inspire the specific utilization of nanozymes as APX mimics in biotherapeutic fields. Besides Cu–N_x, POD-like reactions could also be influenced by the other M–N coordination sites. Zhuang's group demonstrated the ability of M–N (M = Fe, Co, Mn, Ni, and Cu) to produce active M═O intermediates, and the reactivity of substrates at the M═O sites jointly determined the oxidation reaction's selectivity. Remarkably, in catalytic reactions, SANs like Fe–N–C and Co–N–C displayed up to a 200-fold difference in selectivity, surpassing the performance of the frequently employed HRP.[116] Wang *et al.* demonstrated the correlation between the coordination environment of molybdenum (Mo) single-atom sites and POD-like specificity in SANs by designing a series of MoSA–N_x–C nanozymes with different Mo–N_x coordination numbers (Fig. 8aA).[117] MoSA–N_3–C exhibited exclusive POD-like activity and is used for selective analysis of xanthine in human urine samples. Mo–N_3 moiety exhibited better catalytic activity due to its lower energy input, and MoSA–N_3–C displayed the highest H_2O_2 adsorption energy and $\Delta E_{ads.}$ values among Fe–N_3, Co–N_3, Ni–N_3, and Mo–N_3 structures, indicating their high efficiency and specific POD-like performance (Fig. 8aB and C). Zhang *et al.* developed SANs of RhN_4, VN_4, and Fe–Cu–N_6 with catalytic activities surpassing natural enzymes.[118] Furthermore, Rh/VN_4 preferably formed an Rh/V–O–N_4 active center to decrease reaction energy barriers and mediates a "two-sided oxygen-linked" reaction path (Fig. 8b), showing 4 and 5-fold higher affinities in POD-like activity than the FeN_4 and natural HRP.[119] RhN_4 presented a 20-fold improved affinity in the CAT-like activity compared to the natural CAT; Fe–Cu–N_6 displayed selectivity towards the SOD-like activity; VN_4 favored a 7-fold higher GPx-like activity than the natural GPx.

Although SANs with defects have shown great potential in improving reaction selectivity, there are still several limitations that need to be addressed. Achieving high selectivity for SANs may require careful consideration of various factors such as the central atoms, atomic geometrical structure, coordination number, and coordination atoms, which all play a significant role in determining the catalytic activity and selectivity.[120] To fully realize the potential of SANs, efforts are needed to

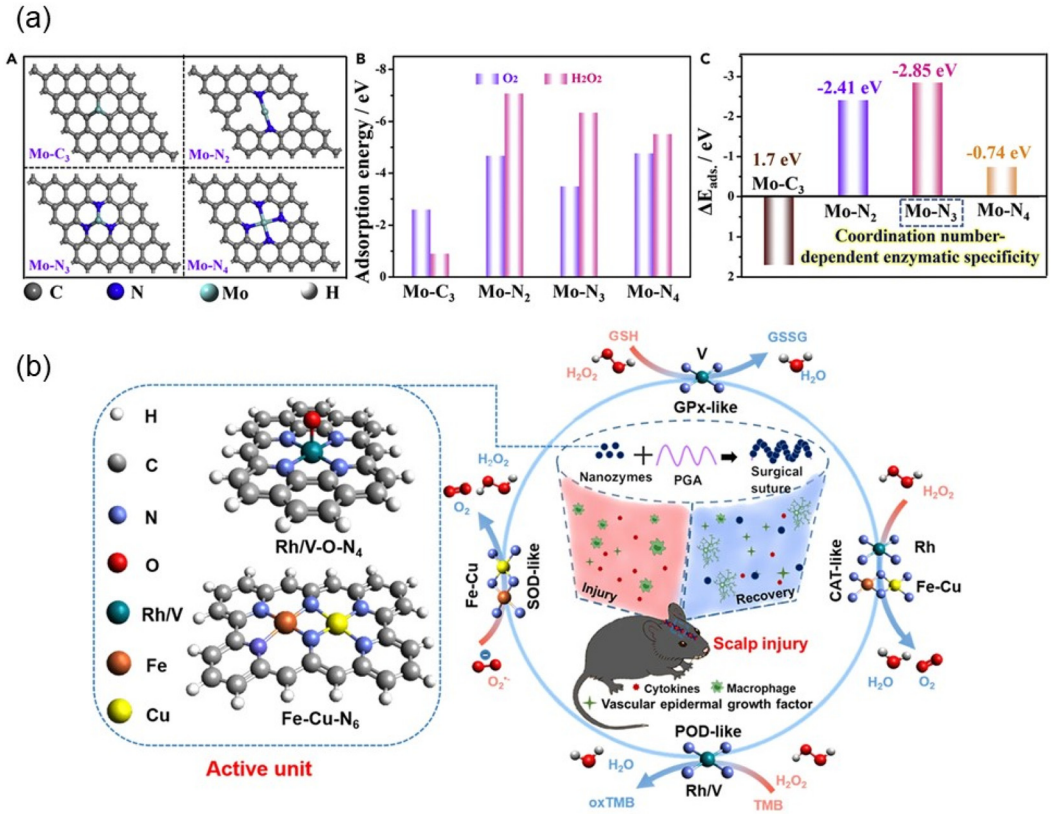

Fig. 8 (a) Construction of selective POD-like Mo SANs: (A) various potential POD-like models with optimized top structures; (B) adsorption energies for O_2 and H_2O_2 on Mo–C_3, Mo–N_2, Mo–N_3, and Mo–N_4 structures; (C) differential values between H_2O_2 and O_2 adsorption energies on Mo–C_3, Mo–N_2, Mo–N_3, and Mo–N_4 structures. Adapted with permission from ref. 117. Copyrights 2021, Elsever. (b) Various active units result in differing activity levels within SANs, which find application in brain trauma healing through the promotion of vascular endothelial growth factor expression and the reduction of oxidative stress and inflammation. Adapted with permission from ref. 118. Copyright 2022, the authors.

address the challenges and limitations associated with their synthesis process. The synthesis process can lead to significant variations in the size and shape of the supported metal species, resulting in variations in their catalytic selectivity. Moreover, SANs are prone to oxidation or dissolution over time, which can affect their stability and selectivity. Additionally, their high cost and strict synthesis conditions can limit their use when compared to traditional enzymes or other types of nanozymes. Many SANs lack biocompatibility and water solubility, further limiting their use in biocultures. Therefore, it is essential to further optimize the methods to synthesize SANs with improved stability, selectivity, and biocompatibility, to fully realize their potential as efficient and effective nanozymes. The SANs may achieve specificity in theranostics through their precisely engineered atomic structure, tunable catalytic activity, surface functionalization, biomimetic design, and multifunctional integration.

4.3 Selective nanomaterials

Among the various types of nanozymes, some unique nanomaterials exhibit exceptional enzyme-like specificity without requiring complicated modification. One such example is Os nanozyme.[121] Compared to conventional noble metal-based nanozymes such as Pt and Au, the POD-like activity of Os nanozyme is considerably high, while its OXD-like activity is negligible. This specificity as a POD mimic facilitates the development of colorimetric sensors to be free from O_2 and color interference in a nanozyme-based colorimetric assay. Moreover, the catalytic selectivities of these nanomaterials can be further modulated by changing their physicochemical properties. CeO_2 nanospheres with specific shapes have been reported to mimic phosphatase and POD-like activities. Tan *et al.* found that acidic Ce species on the octahedron (111) surface selectively catalyze substrate dephosphorylation, while the electron-rich counterpart on the cube (100) surface only promotes substrate oxidation (Fig. 9a).[122] Surface Ce species on the cube have a higher electron density, promoting POD-like activity with ~10 and ~49 times higher reactivity than those on the sphere and octahedron surfaces, respectively. Zhang's group has achieved the selectivity of nanozymes through ingenious HOMO/LUMO-mediated strategies, eliminating the need for additional modifications (Fig. 9b).[123] Their groundbreaking approach involved developing chitosan-coated Se nanozymes with a remarkable 23-fold increase in antioxidative activity compared to Trolox, and bovine serum albumin-coated Te nanozymes with intensified prooxidative biocatalytic effects. This study introduces a pioneering strategy for enhancing the catalytic prowess of Se and Te nanozymes, transcending the boundaries of conventional modifications. These nanomaterials exhibit selectivity without the need for complex modifications, making them highly promising for a broad array of straightforward appli-

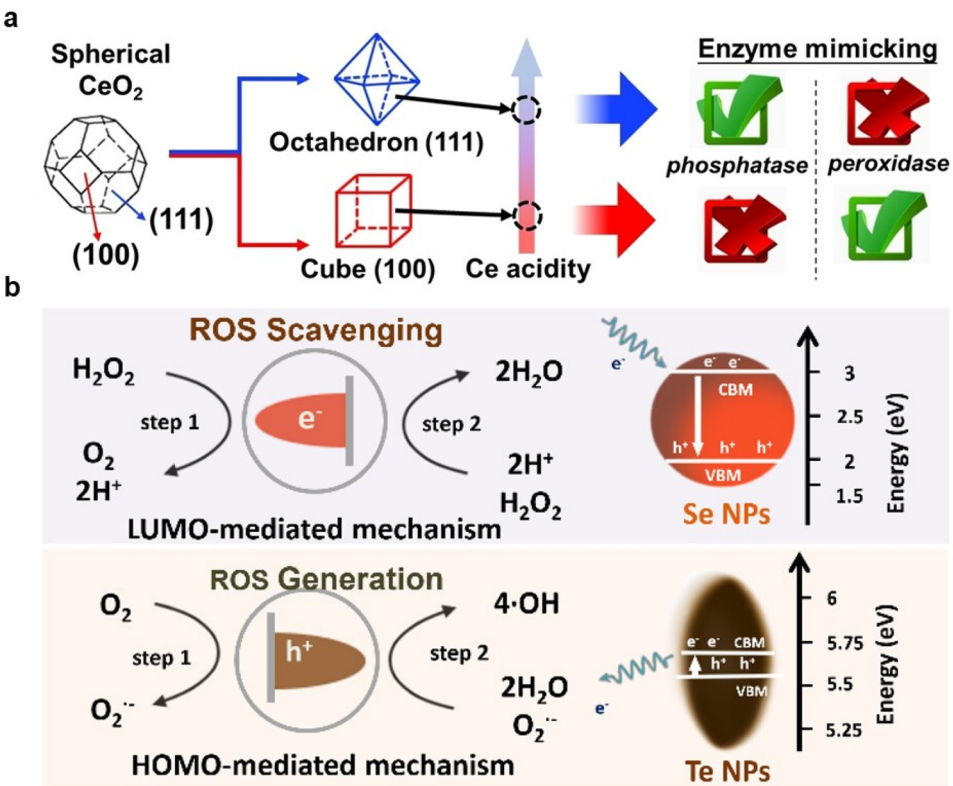

Fig. 9 (a) Shape Regulation of CeO_2 Nanozymes regulates reaction specificity. Adapted with permission from ref. 122. Copyrights 2022, Wiley-VCH GmbH. (b) Catalytic selectivity of LUMO-mediated Se and HOMO-mediated Te. Adapted with permission from ref. 123. Copyrights 20233, ACS.

cations, such as selective biosensing, drug delivery, and environmental remediation.

5. Comprehensive selectivity improvement

Several versatile methods can be harnessed to not only modulate the activity selectivity of nanozymes but also to bolster the selectivity when it comes to analyte detection. A particularly noteworthy approach involves the meticulous regulation of the nanozyme's surface characteristics, a strategy that can wield a multifaceted impact. This regulation has the potential to influence the recognition of analytes, induce the formation of defective nanozyme structures, or even prompt alterations in the internal structure of the nanozyme's active space. It is essential to emphasize that these methods do not solely target a singular aspect of selectivity but rather embrace a holistic approach to refining the nanozyme's performance in diverse applications.

5.1 Stimuli-responsive selectivity

The operating conditions of the reaction, such as light, pH, and temperature, may influence the selectivity of the nanozymes.[124] For instance, upon light irradiation, these materials can undergo structural changes that expose or conceal the active sites of the nanozymes, leading to changes in activity, substrate, and analyte selectivity. Liu *et al.* developed three photoactive MOF-based nanozymes (2D-TCPP, 3D-TCPP, and AD-TCPP) with different structures and unshielded active sites.[125] All three nanozymes exhibited light-responsive OXD-like activities and efficient controllability. These nanozymes exhibited excellent photoresponsive OXD-like activities and substrate specificity for typical oxidase substrates, organic pollutants, and antioxidants. A TiO_2 nanochannel arrays-based membrane (TiNM) was used to create a selective biomolecule detection device by designing a target-molecule triggered recognition event that enabled the growth of POD-like nanozyme Prussian blue nanoparticles (PBNPs) through photocatalytic reaction.[126] The resulting POD-like activity of PBNPs was utilized to detect telomerase activity based on the change in ionic transport behavior induced by the accumulation of positively charged oxTMB molecules in nanochannels. Tian *et al.* discovered that UV light enhances selectivity in porous nanorods of ceria (PN-CeO_2), which exhibit photolyase-like activity.[127] These nanorods selectively cleave UV-formed DNA cyclobutane pyrimidine dimers (CPDs) under visible light. Unlike TiO_2 and ZnO, PN-CeO_2 avoids CPD fragmentation through ROS generation. It retains 91.7% activity even after five cycles and performs better with EDTA due to improved electron–hole separation. PN-CeO_2's unique photocatalytic role in converting CPDs to monomers holds potential for DNA photorepair, akin to natural photolyases. As well as this, graphene oxide (GO) demonstrates notable DNA cleavage activity and selectivity.[128] Remarkably, this process is highly efficient when driven by light, enabling the cleavage of DNA molecules with diverse lengths, ultimately resulting in the formation of the desired products. C-dots demonstrate efficient photo-oxidation correlated with phosphorescence quantum yields, guiding rational design (Fig. 10a).[129] These superior C-dots outperform other carbon nanomaterials and molecular photosensitizers, swiftly driving oxidation reactions. Their potent photosensitized oxygen activation holds promise for applications like photodynamic antimicrobial therapy. Liu's group further improved nanozyme selectivity using C-dots to generate singlet oxygen, converting Mn(II) to Mn(III), and acting as a mediator, selectively enhancing electron transfer for sensitive Mn(II) detection (Fig. 10b).[130] Mn(II) also facilitated substrate oxidation through photosensitized $^1O_2$ production at physiological pH, broadening substrate applicability. This progress drove exploration in biological contexts, addressing pH limitations. In a different vein, the same group discovered the production of $^1O_2$ *via* an Mn^{2+}-mediated system, distinct from the heavy atom effect of Ln^{3+} on photosensitizers (Fig. 10c).[131] Ln^{3+} enhanced $^1O_2$ emission in C-dots and rose bengal four-fold, while nonphosphorescent but fluorescent dyes produced $^1O_2$ mediated by Ln^{3+}. Ln^{3+} also boosted graphene quantum dots, GO, and g-C_3N_4, demonstrating high photocatalytic activity. Fan *et al.* demonstrated that anchoring nano hooks onto Ni@ZIF67-C materials could enrich the superficial N-doped carbons and metal-N_x sites, leading to enhanced POD-like activity.[132] Additionally, Ni@Co–NC exhibited pH-selective and NIR-enhanced POD-like performance. Hong *et al.* investigated the pH-controllable N- and B-doped fullerenes (N-fullerene and B-fullerene) as potential metal-free nanozymes.[133] Under neutral pH conditions, both N- and B-fullerenes with bare surfaces demonstrated dominant POD-like H_2O_2 decomposition activity. The B-fullerene exhibited POD-like activity under solvation at neutral pH. In acidic and basic environments, both N- and B-fullerenes showed dual-enzyme-like functionality, which could be tuned by pH conditions. These findings suggest that fullerene-based nanozymes have pH-dependent enzyme-like activity and selectivity for H_2O_2 decomposition.

The CeO_2 nanoparticles embedded in N-doped carbon (CeO_2@NC) nanozyme has been found to exhibit excellent performance in catalyzing hydrolysis reactions at low temperatures, while CeO_2 NPs do not show enzyme-like properties until high temperatures are reached.[134] The exceptional performance of the CeO_2@NC nanozyme is attributed to the Ce(IV)/Ce(III) species that serve as active sites for polarization and hydrolysis of P═O bonds and the NC template that acts as synergistic sites for substrate adsorption. These discoveries not only provide highly efficient nanozymes with appropriate stimuli but also highlight the need to address several challenges to fully realize the potential of stimuli-responsive selectivity of nanozymes. Overall, stimuli-responsive selectivity in nanozymes offers several advantages in theranostics. By incorporating stimuli-responsive elements, nanozymes can achieve controlled drug release, enhance imaging contrast, function as smart biosensors, enable controlled biochemical reactions, and support personalized therapeutics. On the other hand, one of the major challenges is designing nanomaterials

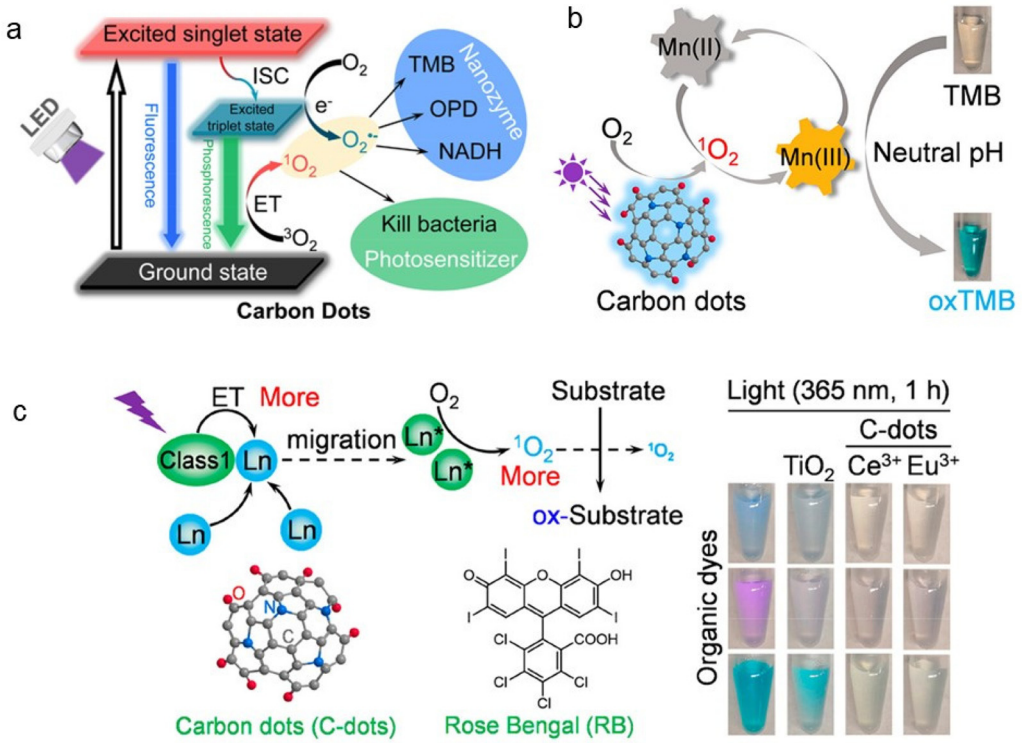

Fig. 10 (a) The catalytic production of oxygen activation by C-dots triggered by light and antimicrobial photodynamic inactivation. Adapted with permission from ref. 129. Copyrights 2018, ACS; (b) the enhancement of photo-OXD activity of C-dots at neutral pH by Mn(II) and the reaction of TMB oxidation. Adapted with permission from ref. 130. Copyrights 2019, ACS; (c) schematic illustrating Ln-enhanced singlet oxygen production using various photosensitizers, as well as powerful photocatalytic oxidation; the photographs depict the effects of TiO_2 and C-dots on four dyes, both in the presence (1 mM Ce^{3+} and 5 mM Eu^{3+}) and absence of light (365 nm, 1 h) at neutral pH. Adapted with permission from ref. 131. Copyrights 2019, ACS.

that can respond to specific stimuli, which requires a deep understanding of the interactions between nanomaterials and stimuli, as well as the underlying mechanisms of the response. Additionally, there are limitations to studying the real-time change of stimuli-responsive nanozymes. For instance, it may be difficult to understand the conformational changes or structural dynamics of nanomaterials in response to stimuli. Additionally, expanding reaction types remains crucial, as most stimuli-activated nanozymes mimic oxidases.[135] Thus, further research is required.

5.2 Surface modification

Surface modification strategies play a pivotal role in reshaping the characteristics and functions of diverse surfaces, underpinned by distinct mechanisms.[136–139] These mechanisms encompass both chemical bonding-based and non-covalent modifications.[140] Peptides, for example, emerge as a captivating pathway for engineering nanozymes, and may rely on precise functional regulation facilitated by supramolecular non-covalent interactions.[141] Beyond peptides, a myriad of strategies have been harnessed to enhance nanozyme's selectivity.

Recent publications spotlight two prominent methods for modification: DNA-based techniques and Molecularly Imprinted Polymers (MIPs). DNA-based approaches harness the versatility of DNA molecules for surface modification, encompassing both covalent bonding and non-covalent interactions. DNA serves multifaceted roles in these strategies, functioning as templates, structural regulators, or recognition elements when coupled with nanozymes. Molecularly Imprinted Polymers (MIPs) primarily rely on non-covalent interactions. Within MIPs, the polymer creates complementary cavities or binding sites that interact with the template molecule through non-covalent mechanisms, such as hydrogen bonding, van der Waals forces, and electrostatic interactions. While MIPs themselves leverage non-covalent interactions to achieve selective binding of target molecules, their collaboration with nanozymes may involve distinct interaction mechanisms.

5.2.1 DNA modification. Harnessing the unique properties of DNA allows for the creation of highly selective nanozymes tailored to specific applications. Various strategies have been proposed to achieve this objective. One such strategy involves using DNA as a template to synthesize DNAzymes and nanozymes with specific structures and surface conditions.[142] DNA templates can guide the covalent bonding of building blocks to form a specific structure. By involving DNA sequences with specific recognition capabilities, precise targeting of disease-

related DNA or RNA molecules is achievable. Another strategy is the modification of the surface of non-selective nanozymes through non-covalent attachment using DNA aptamers to construct selective nanozymes.[143] The aptamer moiety is designed to recognize disease-specific biomarkers, such as proteins or other molecules, allowing the nanozyme to selectively bind and catalyze reactions only in the presence of the target biomarker.

DNAzymes, also known as deoxyribozymes or catalytic DNA, endowed with the remarkable capability to catalyze specific chemical reactions. As an illustration, researchers employed *in vitro* selection techniques to pinpoint a DNAzyme responsive to metal ions. In a series of iterative amplification rounds, they evolved DNA sequences capable of catalyzing Pb^{2+}-dependent cleavage of an RNA phosphodiester bond.[144] Additionally, Li *et al.* harnessed DNAzymes with hydrolytic cleavage activity to create a Pb^{2+} sensor.[145] Moreover, through the integration of DNAzyme and nanozyme specificity and activity, opportunities arise for their strategic design and engineering to enhance reaction selectivity. Zuo *et al.* introduced an inventive approach involving the modification of AuNPs with DNAzymes, leading to the development of highly efficient and selective nanozymes.[146] They utilized a DNA hairpin with two poly(adenosine) internal loops in its stem to bind with AuNPs and form a corona structure, resulting in the creation of novel coronazymes (Fig. 11aA). The coronazymes exhibited 5 times higher catalytic efficiency than bare AuNP nanozymes and outperformed most DNAzymes in the same oxidation reaction. The researchers found that 5 nm bare AuNPs had almost identical catalytic efficiency in *N*-deoxygenation of resazurin (RZ) reduction and amplex red (AR) oxidation, indicating a lack of specificity (Fig. 11aB). However, the coronazymes did not significantly enhance catalytic efficiency in RZ reduction. These results suggest that optimizing the nanozyme using DNAzyme with a corona structure could lead to improved activity selectivity. Mei *et al.* found that the POD-like activity of Pt nanozymes was significantly boosted in the presence of T-rich DNA sequences, showcasing bidirectional regulation (Fig. 11b).[147] This DNA-mediated enhancement extended to stability, with DNA-encoded Pt nanozymes displaying increased robustness against high temperatures, freezing, and prolonged storage. This research's practical application involved creating a sensor array with Pt nanozymes, exhibiting exceptional accuracy in distinguishing antioxidants.

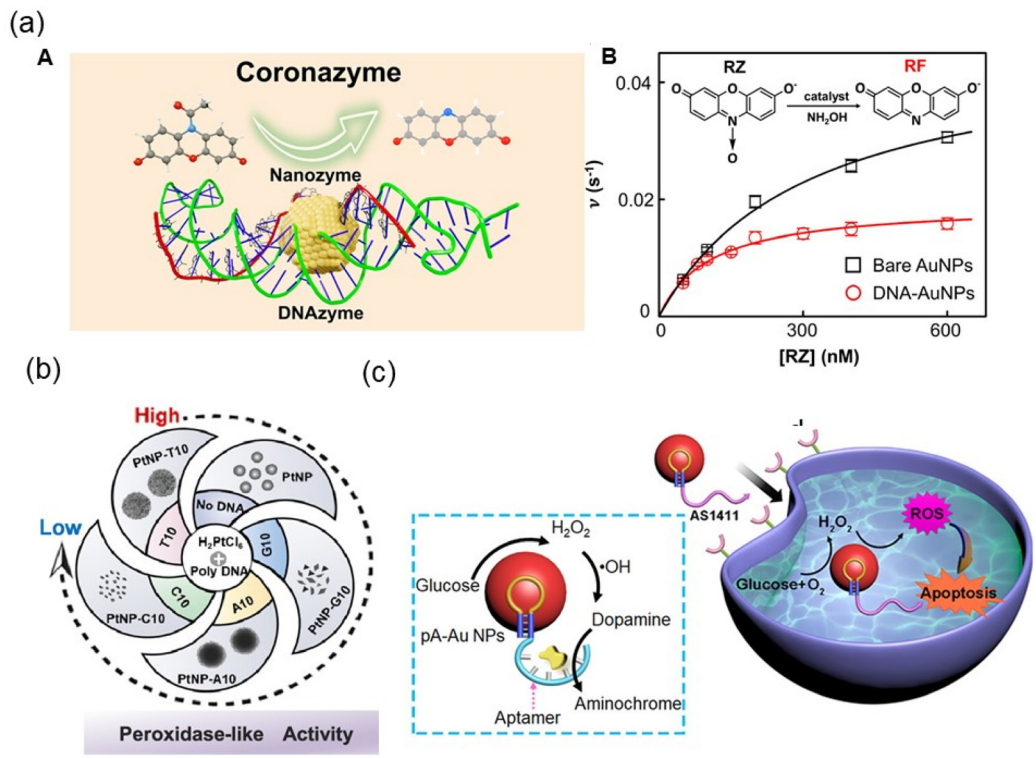

Fig. 11 (a) Selectivity improvement by coronazyme: (A) the integration of DNAzymes and gold nanozymes to form a coronazyme (DNA@AuNPs); (B) the cornazyme does not mimic the dehydrogenase-like reaction; the single-catalyst turnover rate ν was examined as a function of [RZ] for the nanozyme-catalyzed reaction, using NH_2OH for bare AuNPs and DNA@AuNPs. The chemical equation for the *N*-deoxygenation RZ reduction is provided in the inset. Adapted with permission from ref. 146. Copyrights 2023, ACS. (b) DNA-directed bidirectional control of Pt nanozyme's POD-like activity for bioanalysis, T-rich DNA enhances selective POD-like Activity. Adapted with permission from ref. 147. Copyrights 2023, ACS. (c) pA-AuNPs nanoparticles exhibit dual nanozyme catalytic functions involving H_2O_2-mediated oxidation of dopamine to aminochrome and aerobic oxidation of glucose to gluconic acid and H_2O_2. The modification with AS1411 aptamer enhances the nanozyme's selectivity for targeting cancer cells. Adapted with permission from ref. 148. Copyrights 2022, ACS.

DNA aptamers have been employed to enhance analyte selectivity. Ouyang *et al.* ingeniously designed aptananozyme bioreactors, augmenting the activity and selectivity of polyadenine-stabilized Au nanoparticles (pA-AuNPs) by directly attaching dopamine-binding aptamers (DBAs) to their 3′- or 5′-ends or *via* spacer units (Fig. 11c).[148] These pA-AuNPs exhibit dual catalytic functions as nanozymes, participating in both H_2O_2-mediated dopamine oxidation to aminochrome and the aerobic oxidation of glucose to gluconic acid and H_2O_2. To create a nanozyme for targeted chemodynamic cancer treatment, the AS1411 aptamer, which recognizes the nucleolin receptor on cancer cells, is integrated with pA-AuNPs. AS1411 guides the aptananozymes to cancer cells, facilitating selective entry and revealing notable cytotoxicity towards MDA-MB-231 breast cancer cells (approximately 70% cell death) compared to MCF-10A epithelial cells (approximately 2% cell death).

The covalent modifications of nanozymes using thiolated, aminated, and phosphate DNA require additional binding procedures that may influence analyte selectivity. To overcome this limitation, Wei *et al.* developed novel polyadenine-containing diblock DNA as a capping agent for one-pot synthesis of nanoflower-shaped gold nanostructures (AuNFs).[110] The AuNFs exhibited notable POD-like selectivity, rendering them suitable for deployment in colorimetric assays for cancer cell detection. This functionality arises from the combined attributes of the recognition block (aptamer) and the photothermal performance exhibited by the polyadenine block. Compared to spherical gold nanostructures (AuNSs), AuNFs also demonstrated higher sensitivity for the cancer cell assay, enabling the detection of as low as 10 cells per mL. Fu *et al.* utilized bimetallic nanozyme Fe_2MoO_4 NPs in combination with hybridization chain reaction (HCR) to analyze PSCA rs2294008 as a risk factor for bladder cancer prediction.[149] Amplification of absorbance variation and selectivity was achieved by HCR, leading to prolonged DNA length beyond the range of $^{\bullet}OH$ action and double chain with more negative charge to occupy more TMB while repelling the negatively charged nanozyme. This method achieved POD-like selectivity and allowed specific detection of the DNA mutation, which is superior or comparable to most previously reported colorimetric sensors.

Moreover, DNA modification can be utilized as a regulator of nanozyme selectivity by incorporating stimuli-responsive elements that react to specific signals.[150–152] For instance, DNA modification can be employed to create switchable nanozymes that remain inactive under normal conditions but can be activated in response to specific triggers. By incorporating switchable DNA components, such as aptamers or DNA strands with specific secondary structures, the nanozyme can be designed to respond to stimuli such as pH, temperature, or the presence of particular molecules.[153,154] This trigger-dependent activation ensures that the nanozyme exhibits catalytic activity only in the desired disease environment, improving selectivity and minimizing off-target effects.

It's important to note that the field of DNA-modified nanozymes is still advancing, and ongoing research and development efforts are exploring various modifications and strategies to further improve their selectivity and efficacy in theranostics. The DNA molecules may bind non-specifically to the surface of the original nanozymes, leading to the production of unfavorable products that can affect their catalytic activity. Furthermore, the DNA corona structure may degrade in biological environments due to the presence of nucleases, reducing the lifespan of the nanozymes. Despite these challenges, DNA modification presents new opportunities for comprehensively improving the selectivity of nanozymes. For instance, site-specific DNA modifications can be employed to achieve precise control over the selectivity of modified nanozymes. Additionally, the use of stable 3D DNA models for modifying nanozymes may enhance their stability. Nevertheless, the high cost and complexity of DNA engineering remain a concern for the large-scale production of DNA-modified nanozymes.

5.2.2 Molecularly imprinted polymers or particles (MIPs). Molecularly imprinted polymers or particles (MIPs) are synthetic materials that are designed to have specific binding sites for target molecules. MIPs can be tailored to selectively bind to certain analytes due to their molecular recognition properties, similar to antibodies in the immune system.[155] The use of MIPs may significantly improve the analyte, substrate, and activity selectivity of nanozymes.[156] The construction strategies include imprinting transition state molecules, post-imprinting modification, opening cross-linked polymers' internal space, one-pot synthesis, and some special preparation methods (Table 2). For instance, Wu *et al.* showed that g-C_3N_4 has photo-OXD activity, and improved activity selectivity can be achieved by MIPs on g-C_3N_4 nanozymes.[157] MIP-g-C_3N_4 led to over 1000-fold matrix-interference alleviation, 4-fold improved enzymatic activity, and enhanced substrate specificity compared to bare g-C_3N_4 in colorimetric sensing. Peng *et al.* synthesized Co_3O_4-biomass-derived porous carbon (PC) nanocomposites by calcining.[158] They then created the Glu-CS/Co_3O_4-PC electrode by electrodeposition in a mixed solution, and later prepared MIP-Glu-CS/Co_3O_4-PC by eluting glucose electrochemically. This MIP-modified nanozyme shows higher analyte selectivity toward glucose specifically. Chen *et al.* developed DSMIP@Mn_3O_4, a smart tetracycline (TC) imprinted material, using atom transfer radical polymerization of dual ionic liquid monomers on the surface of Mn_3O_4 NPs.[159] The introduction of MIP modification has a dual effect: it inhibits the OXD-like reaction while preserving the POD-like activity. This modulation serves to diminish the generation of $^{\bullet}OH/O_2^{\bullet-}$, consequently leading to a reduction in the production of blue oxTMB. Consequently, this strategic adjustment paves the way for the establishment of an exceptionally selective colorimetric method for the detection of TC. Zhang *et al.* developed a rapid visible analysis method for glycoproteins using a unique ELISA-like satellite structure immunosandwich (SS-ICS) colorimetric strategy.[160] The SS-ICS contained two engineered materials: the boric acid affinity-oriented magnetic titanium dioxide molecularly imprinted particles (MTi-MIP) and the asymmetrically modified Janus gold NPs nanozyme (J-GNPsNE). The MTi-MIP was used as an

Table 2 The performance of recently developed MIPs in enhancing the selectivity of nanozymes

Nanozymes	Printed polymer/ template	Enzyme-like activity	Method	Application	Ref.
MIL-53(Fe)	PDA/MNZ	POD	Self-polymerization	Analysis of MNZ	161
Fe-MOF	CMIP/TCC	POD	Sol–gel method	TCC detection	162
Fe_3O_4 NPs, Au NPs, and Nanoceria	Nanogel/TMB, ABTs	POD	Aqueous precipitation polymerization	Specificity improvement for inorganic nanozymes	163
Fe_3O_4	PDA/TC	POD	Self-polymerization	TC detection	164
MVSM	MIP-2/UA	Uricase	Two-step synthesis	Reduce UA	39
MIL-101(Co,Fe)	PC/vanillin	POD	Chemical cross-linking reaction	Dexamethasone and prednisone detections	23

MNZ, metronidazole; PDA, polydopamine; TCC, triclocarban; CMIP, the capillary molecularly imprinted polymer used in this article is based on Fe-MOF (Fe-MOF@CMIP), which was synthesized by the sol–gel method; TC, tetracycline; AGEC-TCA, termed affinity gathering-enhanced coupling and thermal cycling amplification; MVSM, mixed valence state MOF; UA, uric acid; MIP-2, MIP-2 synthesized using a "two-step synthesis" method involving monomer acrylamide (AM), *N*,*N*′-methylenebisacrylamide (MBAA) and Ce-MOF. PC, a polymer prepared by using a functional monomer immobilized by metal chelation and hydrogen bonding.

"artificial antibody", while J-GNPsNE acted as a target recognition and signal amplification unit. This method enhances the selectivity for analyzing glycoproteins. The integration of MIPs with nanozymes provides a powerful approach for achieving highly specific and efficient catalytic processes. This selectivity, combined with catalytic activities and imaging capabilities, makes MIP-based nanozymes promising tools for theranostics, offering personalized and precise diagnosis, therapy, and monitoring of various diseases. However, the MIP may limit the direct interaction between substrates and active sites exposed on the surface of the nanozyme, which can reduce the efficiency of the catalytic process. To overcome these limitations, various approaches are worth to be further developed to optimize the design of MIP-nanozymes.[111,151] For example, advances in computer-aided design may facilitate the rapid and efficient optimization of MIP for different substrates or targets.

5.3 Cascade nanozyme system

A cascaded nanozyme system can improve reaction specificity by incorporating multiple nanozymes with different enzymatic activities in a sequential manner. Each nanozyme in the cascade performs a specific enzymatic reaction, and the product of the first reaction becomes the substrate for the subsequent reaction (Fig. 12a).[165] A cascade nanozyme system can be designed to exhibit analyte selectivity, substrate selectivity, and control over the activity of nanozymes, depending on their specific configuration and components. For instance, Zhou *et al.* developed a spatially confined microfluidic device for a two-step cascade reaction using N-doped carbon (N–C) nanocages and PB nanoparticles as nanozymes.[166] The overall selectivity of the reactions was substantially improved when N–C and PB nanozymes were cascaded. The system showed high selectivity in the oxidation of AA against interferences, and the efficiency was more than 100-fold higher compared to an open reaction system. The selectivity enhancement even surpassed those in previous reports by at least one order of magnitude, showing the operation principle of substrate channeling and screening in living can also be facilely mimicked with remarkable efficiency.

The sequential reaction process is designed to streamline the identification of target substrates while excluding unwanted interferences through well-suited stimuli, particularly under favorable pH conditions. To exemplify this, the Fe_3O_4–GO_x exhibits inherent capacities akin to glucose OXD (GO_x), CAT, and POD, enabling it to execute pH-triggered cascade reactions initiated by glucose.[167] These encompass GO_x/POD and GO_x/CAT reactions in both acidic and neutral environments. Specifically, in the context of the GO_x/POD cascade reaction, a sequence of hydroxyl radical fluxes is generated to target the acidic biofilm at a pH of approximately 5.5, effectively eradicating it and initiating wound healing by curtailing the inflammatory phase. Conversely, the GO_x/CAT cascade reaction produces successive O_2 fluxes that focus on the neutral wound tissue, thereby expediting the proliferation and remodeling stages. Zhang *et al.* utilized neutral pH H_2O_2 reactions to fabricate nanoceria, demonstrating potent oxidative activity at pH 7.0. This effect is further heightened by protein-induced desorption of oxidation products.[168] Moreover, capitalizing on the negatively charged attributes of BSA and GO_x, with respective isoelectric points of 4.7 and 4.2, fosters favorable interactions with oxTMB and oxOPD, augmenting OPD oxidation while curbing the oxABTS reaction. This strategic approach enables an optimal catalytic cascade involving GO_x and nanoceria at 37 °C and pH 7.0, building upon previous catalytic achievements for targeted serum glucose detection. The selectivity of the nanozyme hinges on a cascade mechanism involving TMB, C-dots, and Sc^{3+} ions.[169] Initially, TMB oxidation was confined to pH 4.0–5.0 when combined with C-dots. However, Sc^{3+} infusion remarkably intensified TMB oxidation across all pH levels, yielding 20-fold higher oxTMB absorbance than C-dots alone. This unique enhancement resulted solely from the Sc^{3+}–C-dots interaction. Additionally, irradiation time was shown to gradually transition TMB oxidation products from a blue to a green solution, indicative of the cascade's role in achieving substrate selectivity and oxidation.

In the domain of chemical reaction networks, a single H_2O_2 stimulus engenders diverse responses with varying intensities

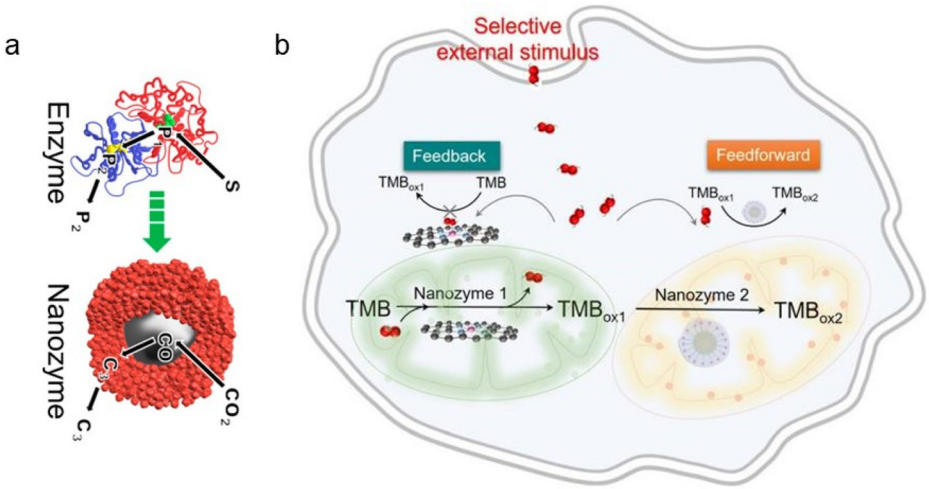

Fig. 12 (a) Scheme highlighting similarities between enzymes that perform cascade reactions. Adapted with permission from ref. 165. Copyrights 2019, ACS. (b) Scheme of the nanozyme-based network of a cascade system. Adapted with permission from ref. 170. Copyrights 2023, RSC.

(Fig. 12b).[170] This phenomenon is exemplified in the two-electron cascade oxidation of TMB, where H_2O_2 concurrently hampers and accelerates reactions within different nanozyme configurations. CeO_2's activation of H_2O_2 and its emulation of POD-like, CAT-like, and haloperoxidase (HPO)-like activities necessitate precise modulation due to the competitive utilization of H_2O_2.[171] Intriguingly, manipulating the H_2O_2 activation pathway on distinct CeO_2 surfaces, such as (100) and (111), fosters specificity towards POD-/CAT-like and HPO-like activities, attributed to the distinct coordination and electronic structures of Ce sites. This research contributes to the comprehensive regulation of nanozyme activity, encompassing selectivity, reaction specificity, and H_2O_2 utilization. These studies highlight the crucial influence of pH conditions and other stimuli in enhancing the selectivity and efficiency of the cascade nanozyme system in biological catalytic processes.

The cascaded nanozyme systems may achieve specificity and selectivity in theranostics by combining complementary catalytic activities, leveraging enzyme-mimicking synergistic effects, enabling targeted therapy, supporting multiplexed detection, and integrating imaging and biosensing capabilities. However, the design of different nanozymes that can work together in a sequential and coordinated manner, reproducibility, stability, characterization, toxicity, and biocompatibility may need to be further addressed.

6. Conclusions

Selective nanozymes hold the key to unlocking a world of possibilities across a diverse range of applications, and ongoing research is focused on enhancing their selectivity through various promising strategies. The summarized strategies, encompassing recognition element introduction, surface modification, precise control of structure and composition, synergistic material synthesis, identification of selective nanomaterials, external stimulus management, and the construction of cascade nanozyme systems, collectively form a robust foundation for enhancing selectivity in specific applications. However, further advancements are necessary to fully exploit the potential of these strategies.

A notable approach involves the development of high-throughput screening methods that empower researchers to efficiently identify the most effective nanozymes for specific reactions and optimize their properties to enhance selectivity. These methods encompass various techniques, including combinatorial chemistry for simultaneous testing of numerous nanozyme compositions, parallel reactor arrays for evaluating multiple nanozymes under various conditions, microfluidic platforms for precise control and rapid screening, computational screening for predicting catalytic activity, and machine learning to facilitate data analysis for uncovering trends and patterns in extensive datasets. Collectively, these techniques expedite nanozyme identification and property optimization, significantly reducing time and resource demands while enhancing catalytic performance for specific reactions. Furthermore, the combination of different strategies, such as the synergistic use of stimuli, defect engineering, surface modification, and more, to enhance nanozymes holds promise in achieving specific reactions. However, careful consideration is essential to balance their interactions and prevent compromising selectivity.

Furthermore, in the pursuit of improved selectivity within complex biological contexts, the development of intelligent nanozymes capable of responding to a broader range of external microenvironmental stimuli holds significant promise. An illustrative example of this approach involves the creation of stimuli-responsive nanozymes for theranostics. Within this context, surface functionalization employing responsive ligands assumes a pivotal role in enhancing adaptability.

Beyond the conventional stimuli widely recognized, such as pH, temperature, and light, considering cellular factors like overexpressed reactive oxygen species holds promise as a valuable parameter for finely modulating the activities of various nanozymes. Furthermore, the incorporation of drug payloads alongside imaging agents not only facilitates precise targeted therapy but also empowers real-time monitoring through a diverse array of imaging techniques.

The pursuit of clinical translation necessitates a strong focus on biocompatibility, safety, and scalability. Meanwhile, personalized medicine approaches should tailor nanozyme designs to the specific disease microenvironment of individual patients. In this intricate optimization process, a multi-dimensional approach is indispensable. By further advancing the selectivity of nanozymes, we can fully unleash the remarkable potential of these nanomaterials, enabling their flexible and diverse applications across a wide range of fields. The ability to selectively target specific molecules, cells, or pathological features will revolutionize diagnostics, therapeutics, and personalized medicine, opening new avenues for precise and effective treatments.

Author contributions

D. Li contributed to writing the original article, and revision. T. Fan contributed to the editing. X. Mei contributed to the supervising of the final manuscript.

Conflicts of interest

There are no conflicts to declare.

Acknowledgements

We acknowledge the financial support from General Project of Natural Science Foundation of Liaoning Province (No. 303202304008).

References

1 C. Peng, R. Pang, J. Li and E. Wang, *Adv. Mater.*, 2023, 2211724, DOI: 10.1002/adma.202211724.
2 Y. Wang, X. Zhang, Y. Dai and F. Xia, *Chem. Eng. J.*, 2023, **455**, 140811.
3 M.-H. Chan, B.-G. Chen, W.-T. Huang, T.-Y. Su, M. Hsiao and R.-S. Liu, *Mater. Today Adv.*, 2023, **17**, 100342.
4 Y. Ma, Z. Tian, W. Zhai and Y. Qu, *Nano Res.*, 2022, **15**, 10328–10342.
5 L. Su, S. Qin, Z. Xie, L. Wang, K. Khan, A. K. Tareen, D. Li and H. Zhang, *Coord. Chem. Rev.*, 2022, **473**, 214784.
6 Y. Wang, A. Cho, G. Jia, X. Cui, J. Shin, I. Nam, K. J. Noh, B. J. Park, R. Huang and J. W. Han, *Angew. Chem., Int. Ed.*, 2023, **62**, e202300119.
7 Y. Liu, B. Wang, J. Zhu, X. Xu, B. Zhou and Y. Yang, *Adv. Mater.*, 2023, **35**, e2208512.
8 J. Sheng, Y. Wu, H. Ding, K. Feng, Y. Shen, Y. Zhang and N. Gu, *Adv. Mater.*, 2023, 2211210, DOI: 10.1002/adma.202211210.
9 Y. Cai, L. Niu, X. Liu, Y. Zhang, Z. Zheng, L. Zeng and A. Liu, *J. Hazard. Mater.*, 2022, **425**, 128053.
10 H. Li, Z. Xiong, Y. Jia, F. Gao, C. Wang, Q. Li and J. Li, *Small*, 2022, **18**, 2202405.
11 T. Zhang, Y. Liu, J. Pi, N. Lu, R. Zhang, W. Chen, Z. Zhang and D. Xing, *Biosens. Bioelectron.*, 2022, **196**, 113686.
12 Y. Lu, C. Cao, X. Pan, Y. Liu and D. Cui, *Nanoscale*, 2022, **15**, 14–40.
13 J. Henych, M. Šťastný, J. Ederer, Z. Němečková, A. Pogorzelska, J. Tolasz, M. Kormunda, P. Ryšánek, B. Bażanów, D. Stygar, K. Mazanec and P. Janoš, *Environ. Sci.: Nano*, 2022, **9**, 3485–3501.
14 Y. Zhao, T. Huang, S. Wang, S. Yao, Q. Hu, X. Wan, N. Guo, Y. Zhang and L. Li, *J. Colloid Interface Sci.*, 2023, **640**, 839–850.
15 B. Li, F. Xia, Y. Liu, H. Tan, S. Gao, J. Kaelin, Y. Liu, K. Lu, T. J. Marks and Y. Cheng, *Nano Lett.*, 2023, **23**, 1459–1466.
16 T. Zhang, N. Lu, C. Wang, R. Zhang, W. Chen, Z. Zhang and D. Xing, *Chem. Eng. J.*, 2022, **437**, 135267.
17 D. Xu, L. Wu, H. Yao and L. Zhao, *Small*, 2022, **18**, 2203400.
18 C. Liu, W. Fan, W. X. Cheng, Y. Gu, Y. Chen, W. Zhou, X. F. Yu, M. Chen, M. Zhu, K. Fan and Q. Y. Luo, *Adv. Funct. Mater.*, 2023, **33**, 2213856.
19 Y. Ai, Z. N. Hu, X. Liang, H. b. Sun, H. Xin and Q. Liang, *Adv. Funct. Mater.*, 2021, **32**, 2110432.
20 S. Zhang, L. Zhang, J. Hu, X. He, B. Geng, D. Pan and L. Shen, *Chem. Eng. J.*, 2023, **458**, 141485.
21 Y. Wang, R. Du, L. Y. S. Lee and K. Y. Wong, *Biosens. Bioelectron.*, 2022, **216**, 114662.
22 X. Mou, Q. Wu, Z. Zhang, Y. Liu, J. Zhang, C. Zhang, X. Chen, K. Fan and H. Liu, *Small Methods*, 2022, **6**, 2200997.
23 Y. Zhang, Y. S. Feng, X. H. Ren, X. W. He, W. Y. Li and Y. K. Zhang, *Biosens. Bioelectron.*, 2022, **196**, 113718.
24 H. Wu, T. Bu, Y. Cao, Y. Wang, J. Xi, M. Li, R. Li, P. Jia and L. Wang, *Anal. Chem.*, 2023, **95**, 5275–5284.
25 A. Bachhuka, T. Chand Yadav, A. Santos, L. F. Marsal, S. Ergün and S. Karnati, *Mater. Today Adv.*, 2022, **15**, 100265.
26 B. Li, H. Shen, Q. Liu, X. Liu, J. Cai, L. Zhang, D. Wu, Y. Xie, G. Xie and W. Feng, *Sens. Actuators, B*, 2023, **386**, 133762.
27 P. Wang, L. Wang, Y. Zhan, Y. Liu, Z. Chen, J. Xu, J. Guo, J. Luo, J. Wei, F. Tong and Z. Li, *Chem. Eng. J.*, 2023, **463**, 142293.
28 X. Ma, J. Hao, J. Wu, Y. Li, X. Cai and Y. Zheng, *Adv. Mater.*, 2022, **34**, 2106723.
29 Z. Zhang and K. Fan, *Nanoscale*, 2022, **15**, 41–62.
30 Q. Wang, C. Cheng, S. Zhao, Q. Liu, Y. Zhang, W. Liu, X. Zhao, H. Zhang, J. Pu, S. Zhang, H. Zhang, Y. Du and H. Wei, *Angew. Chem., Int. Ed.*, 2022, **61**, 202201101.

31 H. Mao, Y. Wen, Y. Yu, H. Li, J. Wang and B. Sun, *J. Mater. Chem. B*, 2022, **11**, 131–143.
32 K. Wu, D. Zhu, X. Dai, W. Wang, X. Zhong, Z. Fang, C. Peng, X. Wei, H. Qian, X. Chen, X. Wang, Z. Zha and L. Cheng, *Nano Today*, 2022, **43**, 101380.
33 G. Fang, R. Kang, S. Cai and C. Ge, *Nano Today*, 2023, **48**, 101755.
34 X. Guo, F. Yang, L. Jing, J. Li, Y. Li, R. Ding, B. Duan and X. Zhang, *J. Hazard. Mater.*, 2022, **431**, 128621.
35 Y. Guan, Y. Lu, J. Zhao, W. Huang and Y. Liu, *Chem. Eng. J.*, 2023, **465**, 142703.
36 D. Chao, Q. Dong, J. Chen, Z. Yu, W. Wu, Y. Fang, L. Liu and S. Dong, *Appl. Catal., B*, 2022, **304**, 142703.
37 C. Chi, W. Zhang, M. Luo, M. Zhang and G. Chen, *Chem. Eng. J.*, 2023, **458**, 141321.
38 S. Dong, Y. Dong, Z. Zhao, J. Liu, S. Liu, L. Feng, F. He, S. Gai, Y. Xie and P. Yang, *J. Am. Chem. Soc.*, 2023, **145**, 9488–9507.
39 D. Liu, S. Yi, X. Ni, J. Zhang, F. Wang, P. Yang, M. Liu, J. Peng, P. Dramou and H. He, *ChemPlusChem*, 2023, **88**, 202200286.
40 X. Ji, Q. Li, H. Song and C. Fan, *Adv. Mater.*, 2022, **34**, 2201562.
41 M. Drozd, A. Duszczyk, P. Ivanova and M. Pietrzak, *Adv. Colloid Interface Sci.*, 2022, **304**, 102656.
42 M. Jiao, Z. Li, X. Li, Z. Zhang, Q. Yuan, F. Vriesekoop, H. Liang and J. Liu, *Chem. Eng. J.*, 2020, **388**, 124249.
43 Q. Liu, X. Zhu, L. Zhong, S. Zhang, X. Luo, Q. Liu, L. Tang and Y. Lu, *Environ. Sci.: Nano*, 2022, **9**, 1212–1235.
44 F. Meng, P. Zhu, L. Yang, L. Xia and H. Liu, *Chem. Eng. J.*, 2023, **452**, 139411.
45 G. Xu, X. Du, W. Wang, Y. Qu, X. Liu, M. Zhao, W. Li and Y. Q. Li, *Small*, 2022, **18**, 2204131.
46 Y. Wu, W. Xu, L. Jiao, Y. Tang, Y. Chen, W. Gu and C. Zhu, *Mater. Today*, 2022, **52**, 327–347.
47 Q. He and L. Zhang, *J. Mater. Chem.*, 2023, **11**, 5071–5082.
48 D. Li, D. Dai, G. Xiong, S. Lan and C. Zhang, *Small*, 2023, **19**, 2205870.
49 D. O. Lopez-Cantu, R. B. González-González, A. Sharma, M. Bilal, R. Parra-Saldívar and H. M. N. Iqbal, *Coord. Chem. Rev.*, 2022, **469**, 214685.
50 Y. Lai, J. Wang, N. Yue, Q. Zhang, J. Wu, W. Qi and R. Su, *Biomater. Sci.*, 2023, **11**, 2292–2316.
51 S. Zhang, R. Zhang, X. Yan and K. Fan, *Small*, 2022, **18**, 2202294.
52 J. Zhuang, A. C. Midgley, Y. Wei, Q. Liu, D. Kong and X. Huang, *Adv. Mater.*, 2023, 2210848, DOI: **10.1002/adma.202210848**.
53 Y. Ouyang, M. P. O'Hagan and I. Willner, *Biosens. Bioelectron.*, 2022, **218**, 114768.
54 Q. Zhang, L. Song and K. Zhang, *Mater. Chem. Front.*, 2023, **7**, 44–64.
55 X. Li, H. Zhu, P. Liu, M. Wang, J. Pan, F. Qiu, L. Ni and X. Niu, *TrAC, Trends Anal. Chem.*, 2021, **143**, 116379.
56 S. V. Somerville, Q. Li, J. Wordsworth, S. Jamali, M. R. Eskandarian, R. D. Tilley and J. J. Gooding, *Adv. Mater.*, 2023, 2211288, DOI: **10.1002/adma.202211288**.
57 P. Huang, C. Wang, H. Deng, Y. Zhou and X. Chen, *Acc. Chem. Res.*, 2023, **56**, 1766–1779.
58 J. Han, H. Li, L. Zhao, G. Kim, Y. Chen, X. Yan and J. Yoon, *Chem. Sci.*, 2022, **13**, 7814–7820.
59 A. Ali, M. Ovais, H. Zhou, Y. Rui and C. Chen, *Biomaterials*, 2021, **275**, 120951.
60 S. Sisakhtnezhad, M. Rahimi and S. Mohammadi, *Biomed. Pharmacother.*, 2023, **163**, 114833.
61 C. Cao, N. Yang, Y. Su, Z. Zhang, C. Wang, X. Song, P. Chen, W. Wang and X. Dong, *Adv. Mater.*, 2022, **34**, 2203236.
62 L. Li, Z. Lin, X. Xu, W. Wang, H. Chen, Z. Feng, Z. Yang and J. Hao, *ACS Appl. Mater. Interfaces*, 2023, **15**, 41224–41236.
63 H. Hu, H. Huang, L. Xia, X. Qian, W. Feng, Y. Chen and Y. Li, *Chem. Eng. J.*, 2022, **440**, 135810.
64 S. Guo, Y. Xiao, Y. Sun, L. Qu, Q. Cai and Z. Li, *Sens. Actuators, B*, 2023, **390**, 133977.
65 F. Liu, L. Lin, Y. Zhang, Y. Wang, S. Sheng, C. Xu, H. Tian and X. Chen, *Adv. Mater.*, 2019, **31**, 1902885.
66 D.-Y. Zhang, H. Liu, M. R. Younis, S. Lei, C. Yang, J. Lin, J. Qu and P. Huang, *Chem. Eng. J.*, 2021, **409**, 127371.
67 Z. Miao, S. Jiang, M. Ding, S. Sun, Y. Ma, M. R. Younis, G. He, J. Wang, J. Lin, Z. Cao, P. Huang and Z. Zha, *Nano Lett.*, 2020, **20**, 3079–3089.
68 H. Wu, F. Xia, L. Zhang, C. Fang, J. Lee, L. Gong, J. Gao, D. Ling and F. Li, *Adv. Mater.*, 2022, **34**, 2108348.
69 X. Jing, L. Meng, S. Fan, T. Yang, N. Zhang, R. Xu, X. Zhao, H. Yang, Z. Yang, D. Wang, Y. Liang, G. Zhou, W. Ji and J. She, *Chem. Eng. J.*, 2022, **442**, 136096.
70 C. Chen, Y. Chen, L. Zhang, X. Wang, Q. Tang, Y. Luo, Y. Wang, C. Ma and X. Liang, *J. Nanobiotechnol.*, 2022, **20**, 466.
71 F. Nan, Q. Jia, X. Xue, S. Wang, W. Liu, J. Wang, J. Ge and P. Wang, *Biomaterials*, 2022, **284**, 121495.
72 T. Jia, D. Li, J. Du, X. Fang, V. Gerasimov, H. Agren and G. Chen, *J. Nanobiotechnol.*, 2022, **20**, 424.
73 G. Zhang, N. Li, Y. Qi, Q. Zhao, J. Zhan and D. Yu, *Acta Biomater.*, 2022, **142**, 284–297.
74 F. Gao, J. Wu, H. Gao, X. Hu, L. Liu, A. C. Midgley, Q. Liu, Z. Sun, Y. Liu, D. Ding, Y. Wang, D. Kong and X. Huang, *Biomaterials*, 2020, **230**, 119635.
75 D. H. Zhao, C. Q. Li, X. L. Hou, X. T. Xie, B. Zhang, G. Y. Wu, F. Jin, Y. D. Zhao and B. Liu, *ACS Appl. Mater. Interfaces*, 2021, **13**, 55780–55789.
76 Y. Liu, L. Chen, Z. Chen, M. Liu, X. Li, Y. Kou, M. Hou, H. Wang, X. Li, B. Tian and J. Dong, *ACS Nano*, 2023, **17**, 8167–8182.
77 L. Yang, H. Zhu, R. Zhao, Z. Zhang, B. Liu, H. Gong, Y. Zhu, H. Ding, S. Gai and L. Feng, *Chem. Eng. J.*, 2022, **450**, 138137.
78 H. Fan, J. Zheng, J. Xie, J. Liu, X. Gao, X. Yan, K. Fan and L. Gao, *Adv. Mater.*, 2023, 2300387, DOI: **10.1002/adma.202300387**.

79 X. Tao, X. Wang, B. Liu and J. Liu, *Biosens. Bioelectron.*, 2020, **168**, 112537.
80 B. Das, J. L. Franco, N. Logan, P. Balasubramanian, M. I. Kim and C. Cao, *Nano-Micro Lett.*, 2021, **13**, 193.
81 F. Zhao, L. Wang, M. Li, M. Wang, G. Liu and J. Ping, *TrAC, Trends Anal. Chem.*, 2023, **165**, 117152.
82 A. Shamsabadi, T. Haghighi, S. Carvalho, L. C. Frenette and M. M. Stevens, *Adv. Mater.*, 2023, 2300184, DOI: **10.1002/adma.202300184**.
83 X. Cai, M. Liang, F. Ma, S. R. Mohamed, A. A. Goda, D. H. Dawood, L. Yu and P. Li, *Anal. Methods*, 2021, **13**, 5542–5548.
84 L. Zhang, H. Wang and X. Qu, *Adv. Mater.*, 2023, 2211147, DOI: **10.1002/adma.202211147**.
85 L. Zhou, Y. Liu, Y. Lu, P. Zhou, L. Lu, H. Lv and X. Hai, *Biosensors*, 2022, **12**, 1119.
86 R. Li, H. Fan, H. Zhou, Y. Chen, Q. Yu, W. Hu, G. L. Liu and L. Huang, *Adv. Sci.*, 2023, **10**, 2301658.
87 X. Wei, S. Song, W. Song, Y. Wen, W. Xu, Y. Chen, Z. Wu, Y. Qin, L. Jiao, Y. Wu, M. Sha, J. Huang, X. Cai, L. Zheng, L. Hu, W. Gu, M. Eguchi, T. Asahi, Y. Yamauchi and C. Zhu, *Chem. Sci.*, 2022, **13**, 13574–13581.
88 P. Ivanova, M. Drozd, K. Michrowski, S. Karon, M. Mazurkiewicz-Pawlicka and M. Pietrzak, *Biosens. Bioelectron.*, 2023, **237**, 115511.
89 Y. Wang and Y. Xianyu, *Small Methods*, 2022, **6**, 2101576.
90 C. Zhang, J. Hu, X. Wu, J. Shi and B. D. Hammock, *ACS Agric. Sci. Technol.*, 2022, **2**, 573–579.
91 Y. Zhou, Y. Wei, J. Ren and X. Qu, *Mater. Horiz.*, 2020, **7**, 3291–3297.
92 Q. Chen, X. Zhang, S. Li, J. Tan, C. Xu and Y. Huang, *Chem. Eng. J.*, 2020, **395**, 125130.
93 Y. Chen, L. Jiao, H. Yan, W. Xu, Y. Wu, L. Zheng, W. Gu and C. Zhu, *Anal. Chem.*, 2021, **93**, 12353–12359.
94 M. Liang, Y. Wang, K. Ma, S. Yu, Y. Chen, Z. Deng, Y. Liu and F. Wang, *Small*, 2020, **16**, e2002348.
95 M. Lian, M. Liu, X. Zhang, W. Zhang, J. Zhao, X. Zhou and D. Chen, *ACS Appl. Mater. Interfaces*, 2021, **13**, 53599–53609.
96 M. Wang, M. Chang, P. Zheng, Q. Sun, G. Wang, J. Lin and C. Li, *Adv. Sci.*, 2022, **9**, 2202332.
97 Y. Tang, Y. Chen, Y. Wu, W. Xu, Z. Luo, H. R. Ye, W. Gu, W. Song, S. Guo and C. Zhu, *Nano Lett.*, 2023, **23**, 267–275.
98 S. Xu, X. Dong, S. Chen, Y. Zhao, G. Shan, Y. Sun, Y. Chen and Y. Liu, *Sens. Actuators, B*, 2019, **281**, 375–382.
99 S. Zhang, J. Chen, W.-S. Yang and X. Chen, *Nano Res.*, 2022, **15**, 7940–7950.
100 C. Shang, Q. Wang, H. Tan, S. Lu, S. Wang, Q. Zhang, L. Gu, J. Li, E. Wang and S. Guo, *JACS Au*, 2022, **2**, 2453–2459.
101 W. Lu, J. Chen, L. Kong, F. Zhu, Z. Feng and J. Zhan, *Sens. Actuators, B*, 2021, **333**, 129560.
102 Y. Song, C. Huang and Y. Li, *Inorg. Chem.*, 2023, **62**, 12697–12707.
103 M. Wang, J. Wang, Y. Hou, D. Shi, D. Wexler, S. D. Poynton, R. C. Slade, W. Zhang, H. Liu and J. Chen, *ACS Appl. Mater. Interfaces*, 2015, **7**, 7066–7072.
104 N. Ye, S. Huang, H. Yang, T. Wu, L. Tong, F. Zhu, G. Chen and G. Ouyang, *Anal. Chem.*, 2021, **93**, 13981–13989.
105 Y. Hu, X. J. Gao, Y. Zhu, F. Muhammad, S. Tan, W. Cao, S. Lin, Z. Jin, X. Gao and H. Wei, *Chem. Mater.*, 2018, **30**, 6431–6439.
106 S. Ding, J. A. Barr, Z. Lyu, F. Zhang, M. Wang, P. Tieu, X. Li, M. H. Engelhard, Z. Feng, S. P. Beckman, X. Pan, J. C. Li, D. Du and Y. Lin, *Adv. Mater.*, 2023, 2209633, DOI: **10.1002/adma.202209633**.
107 J. Lee, H. Liao, Q. Wang, J. Han, J. H. Han, H. E. Shin, M. Ge, W. Park and F. Li, *Exploration*, 2022, **2**, 20210086.
108 H. Liu, Y. Li, S. Sun, Q. Xin, S. Liu, X. Mu, X. Yuan, K. Chen, H. Wang, K. Varga, W. Mi, J. Yang and X. D. Zhang, *Nat. Commun.*, 2021, **12**, 114.
109 T. Wang, J. Feng, H. Sun, Y. Liang, T. Du, J. Dan, J. Wang and W. Zhang, *Sens. Actuators, B*, 2023, **379**, 133249.
110 Z. Wei, Y. Yu, S. Hu, X. Yi and J. Wang, *ACS Appl. Mater. Interfaces*, 2021, **13**, 16801–16811.
111 X. Cheng, X. Zhou, Z. Zheng and Q. Kuang, *Chem. Eng. J.*, 2022, **430**, 133079.
112 C. Zhou, Y. Zeng, Z. Song, Q. Liu, Y. Zhang, M. Wang and Y. Du, *Anal. Chem.*, 2022, **94**, 13261–13268.
113 M. Li, J. Chen, W. Wu, Y. Fang and S. Dong, *J. Am. Chem. Soc.*, 2020, **142**, 15569–15574.
114 M. Chen, H. Zhang, L. Tian, H. Lv, C. Chen, X. Liu, W. Wang, Y. Wang, Y. Zhao, J. Wang, H. Zhou, Y. Mao, C. Xiong and Y. Wu, *ACS Appl. Mater. Interfaces*, 2023, **15**, 407–415.
115 Y. Chen, H. Zou, B. Yan, X. Wu, W. Cao, Y. Qian, L. Zheng and G. Yang, *Adv. Sci.*, 2022, **9**, e2103977.
116 X. Chen, L. Zhao, K. Wu, H. Yang, Q. Zhou, Y. Xu, Y. Zheng, Y. Shen, S. Liu and Y. Zhang, *Chem. Sci.*, 2021, **12**, 8865–8871.
117 Y. Wang, G. Jia, X. Cui, X. Zhao, Q. Zhang, L. Gu, L. Zheng, L. H. Li, Q. Wu, D. J. Singh, D. Matsumura, T. Tsuji, Y.-T. Cui, J. Zhao and W. Zheng, *Chem*, 2021, **7**, 436–449.
118 S. Zhang, Y. Li, S. Sun, L. Liu, X. Mu, S. Liu, M. Jiao, X. Chen, K. Chen, H. Ma, T. Li, X. Liu, H. Wang, J. Zhang, J. Yang and X. D. Zhang, *Nat. Commun.*, 2022, **13**, 4744.
119 L. Huang, J. Chen, L. Gan, J. Wang and S. Don, *Sci. Adv.*, 2019, **5**, eaav5490.
120 H. Jin, D. Ye, L. Shen, R. Fu, Y. Tang, J. C. Jung, H. Zhao and J. Zhang, *Anal. Chem.*, 2022, **94**, 1499–1509.
121 S. He, L. Yang, P. Balasubramanian, S. Li, H. Peng, Y. Kuang, H. Deng and W. Chen, *J. Mater. Chem. A*, 2020, **8**, 25226–25234.
122 Z. Tan, Y. Wang, J. Zhang, Z. Zhang, S. S. Man Wong, S. Zhang, H. Sun, K. K. L. Yung and Y. K. Peng, *Eur. J. Inorg. Chem.*, 2022, **2022**, 202200202.
123 K. Liu, J. Niu, L. Liu, F. Tian, H. Nie, X. Liu, K. Chen, R. Zhao, S. Sun, M. Jiao, M. Tian, X. Sun, L. Niu, X. Sun, H. Wang, W. Long, L. Feng, X. Mu and X. D. Zhang, *Nano Lett.*, 2023, **23**, 5131–5140.
124 X. Chen, J. Liao, Y. Lin, J. Zhang and C. Zheng, *Anal. Bioanal. Chem.*, 2023, **415**, 3817–3830.

125 Y. Liu, X. Wang, Q. Wang, Y. Zhang, Q. Liu, S. Liu, S. Li, Y. Du and H. Wei, *Anal. Chem.*, 2021, **93**, 15150–15158.
126 Z. Dai, J. Guo, J. Xu, C. Liu, Z. Gao and Y. Y. Song, *Anal. Chem.*, 2020, **92**, 10033–10041.
127 Z. Tian, T. Yao, C. Qu, S. Zhang, X. Li and Y. Qu, *Nano Lett.*, 2019, **19**, 8270–8277.
128 J. Zhang, S. Wu, L. Ma, P. Wu and J. Liu, *Nano Res.*, 2020, **13**, 455–460.
129 J. Zhang, X. Lu, D. Tang, S. Wu, X. Hou, J. Liu and P. Wu, *ACS Appl. Mater. Interfaces*, 2018, **10**, 40808–40814.
130 J. Zhang, S. Wu, X. Lu, P. Wu and J. Liu, *Nano Lett.*, 2019, **19**, 3214–3220.
131 J. Zhang, S. Wu, X. Lu, P. Wu and J. Liu, *ACS Nano*, 2019, **13**, 14152–14161.
132 X. Fan, X. Wu, F. Yang, L. Wang, K. Ludwig, L. Ma, A. Trampuz, C. Cheng and R. Haag, *Angew. Chem., Int. Ed.*, 2022, **61**, e202113833.
133 S. J. Hong, H. Chun, M. Hong and B. Han, *Appl. Surf. Sci.*, 2022, **598**, 153715.
134 P. Gai, L. Pu, C. Wang, D. Zhu and F. Li, *Biosens. Bioelectron.*, 2023, **220**, 114841.
135 J. Zhang and J. Liu, *Nanoscale*, 2020, **12**, 2914–2923.
136 X. Zhu, T. Li, X. Hai and S. Bi, *Biosens. Bioelectron.*, 2022, **213**, 114438.
137 L. Su, S. Qin, Y. Cai, L. Wang, W. Dong, G. Mao, S. Feng, Z. Xie and H. Zhang, *Sens. Actuators, B*, 2022, **353**, 131150.
138 M. Zandieh and J. Liu, *Langmuir*, 2022, **38**, 3617–3622.
139 Y. Zhe, J. Wang, Z. Zhao, G. Ren, J. Du, K. Li and Y. Lin, *Biosens. Bioelectron.*, 2023, **220**, 114893.
140 H. Wu, J. Liu, Z. Chen, P. Lin, W. Ou, Z. Wang, W. Xiao, Y. Chen and D. Cao, *Langmuir*, 2022, **38**, 8266–8279.
141 J. Han, H. Gong, X. Ren and X. Yan, *Nano Today*, 2021, **41**, 101295.
142 Z. Wu, W. Liu, H. Lu, H. Zhang, Z. Hao, F. Zhang, R. Zhang, X. Li and L. Zhang, *Nanoscale*, 2023, **15**, 13289–13296.
143 L. Sun, C. Li, Y. Yan, Y. Yu, H. Zhao, Z. Zhou, F. Wang and Y. Feng, *Anal. Chim. Acta*, 2021, **1180**, 338856.
144 R. R. Breaker and G. F. Joyce, *Chem. Biol.*, 1994, **1**, 223–229.
145 J. Li and Y. Lu, *J. Am. Chem. Soc.*, 2000, **122**, 10466–10467.
146 L. Zuo, K. Ren, X. Guo, P. Pokhrel, B. Pokhrel, M. A. Hossain, Z. X. Chen, H. Mao and H. Shen, *J. Am. Chem. Soc.*, 2023, **145**, 5750–5758.
147 W. Mei, W. Huang, X. Liu, H. Wang, Q. Wang, X. Yang and K. Wang, *Anal. Chem.*, 2023, **95**, 11391–11398.
148 Y. Ouyang, M. Fadeev, P. Zhang, R. Carmieli, J. Li, Y. S. Sohn, O. Karmi, R. Nechushtai, E. Pikarsky, C. Fan and I. Willner, *ACS Nano*, 2022, **16**, 18232–18243.
149 Y. Fu, Z. Zhao, Y. Shi, K. Xu, J. Zhang, H. Niu and Y. Xu, *Biosens. Bioelectron.*, 2022, **210**, 114272.
150 M. Mahmoudpour, S. Ding, Z. Lyu, G. Ebrahimi, D. Du, J. Ezzati Nazhad Dolatabadi, M. Torbati and Y. Lin, *Nano Today*, 2021, **39**, 101177.
151 R. Yu, R. Wang, Z. Wang, Q. Zhu and Z. Dai, *Analyst*, 2021, **146**, 1127–1141.
152 Z. Wang, H. Liu, S. H. Yang, T. Wang, C. Liu and Y. C. Cao, *Proc. Natl. Acad. Sci. U. S. A.*, 2012, **109**, 12387–12392.
153 M. Cai, Y. Zhang, Z. Cao, W. Lin and N. Lu, *ACS Appl. Mater. Interfaces*, 2023, **15**, 18620–18629.
154 C. Zeng, N. Lu, Y. Wen, G. Liu, R. Zhang, J. Zhang, F. Wang, X. Liu, Q. Li, Z. Tang and M. Zhang, *ACS Appl. Mater. Interfaces*, 2019, **11**, 1790–1799.
155 R. Tian, Y. Li, J. Xu, C. Hou, Q. Luo and J. Liu, *J. Mater. Chem. B*, 2022, **10**, 6590–6606.
156 L. Fang, M. Jia, H. Zhao, L. Kang, L. Shi, L. Zhou and W. Kong, *Trends Food Sci. Technol.*, 2021, **116**, 387–404.
157 Y. Wu, Q. Chen, S. Liu, H. Xiao, M. Zhang and X. Zhang, *Chin. Chem. Lett.*, 2019, **30**, 2186–2190.
158 C. Peng, L. Miao, D. Qiu and S. Chen, *Ceram. Int.*, 2022, **48**, 23137–23144.
159 Y. Chen, Y. Xia, Y. Liu, Y. Tang, F. Zhao and B. Zeng, *Biosens. Bioelectron.*, 2022, **216**, 114650.
160 Y.-D. Zhang, C. Ma and Y.-P. Shi, *Chem. Eng. J.*, 2023, **454**, 140495.
161 Z. Zhang, Y. Liu, P. Huang, F. Y. Wu and L. Ma, *Talanta*, 2021, **232**, 122411.
162 Y. Chen, K. Tang, X. Wang, Q. Zhou, S. Tang, X. Wu, P. Zhao, H. Lei, Z. Yang and Z. Zhang, *Sens. Actuators, B*, 2023, **382**, 133543.
163 Z. Zhang, X. Zhang, B. Liu and J. Liu, *J. Am. Chem. Soc.*, 2017, **139**, 5412–5419.
164 B. Liu, H. Zhu, R. Feng, M. Wang, P. Hu, J. Pan and X. Niu, *Sens. Actuators, B*, 2022, **370**, 132451.
165 P. B. O'Mara, P. Wilde, T. M. Benedetti, C. Andronescu, S. Cheong, J. J. Gooding, R. D. Tilley and W. Schuhmann, *J. Am. Chem. Soc.*, 2019, **141**, 14093–14097.
166 Q. Zhou, H. Yang, X. Chen, Y. Xu, D. Han, S. Zhou, S. Liu, Y. Shen and Y. Zhang, *Angew. Chem., Int. Ed.*, 2022, **61**, 202112453.
167 X. Du, B. Jia, W. Wang, C. Zhang, X. Liu, Y. Qu, M. Zhao, W. Li, Y. Yang and Y. Q. Li, *J. Nanobiotechnol.*, 2022, **20**, 12.
168 J. Zhang, J. Wang, J. Liao, Y. Lin, C. Zheng and J. Liu, *ACS Appl. Mater. Interfaces*, 2021, **13**, 50236–50245.
169 X. Chen, Y. Lin, J. Liao, J. Zhang and C. Zheng, *J. Mater. Chem. B*, 2023, **11**, 6697–6703.
170 C. Zhu, Z. Zhou, X. J. Gao, Y. Tao, X. Cao, Y. Xu, Y. Shen, S. Liu and Y. Zhang, *Chem. Sci.*, 2023, **14**, 6780–6791.
171 B. Yuan, Z. Tan, Q. Guo, X. Shen, C. Zhao, J. L. Chen and Y. K. Peng, *ACS Nano*, 2023, **17**, 17383–17393.